

# Hyperbolic Knot Theory

Jessica S. Purcell

These notes consist of lectures from a graduate course I taught at Brigham Young University in winter semester 2010. They are somewhat rough, but possibly of interest to others.

The material here is primarily due to W. Thurston. Much of the material is inspired by his notes [19], and a few figures are taken directly from those notes (credited in text). Some material is also inspired by discussion and exercises in his book [21].

I also would like to thank the organizers of the workshop on Interactions between hyperbolic geometry, quantum topology, and number theory held at Columbia University in June 2009. These notes were written while those workshops were still fresh in my mind, and several talks related to these notes. Finally, these notes have also benefitted from discussions with David Futer and Henry Segerman on best ways to describe hyperbolic geometry of knots.

Any errors are, of course, my own. Please let me know about them.

Jessica S. Purcell  
Department of Mathematics  
Brigham Young University  
Provo, UT 84602  
USA  
jpurcell@math.byu.edu

## Contents

Chapter 1. Introduction	5
1.1. Some motivation and history	5
1.2. Basic terminology	6
Chapter 2. Polyhedral decomposition of the Figure–8 knot complement	9
2.1. Introduction	9
2.2. Vocabulary	9
2.3. Polyhedra	9
2.4. Exercises	14
Chapter 3. Hyperbolic geometry and ideal tetrahedra	19
3.1. Basic hyperbolic geometry	19
3.2. Exercises	23
Chapter 4. Geometric structures on manifolds	27
4.1. Geometric structures	27
4.2. Complete structures	32
4.3. Developing map and completeness	39
4.4. Exercises	39
Chapter 5. Hyperbolic structures on knot complements	41
5.1. Geometric triangulations	41
5.2. Gluing equations	45
5.3. Completeness equations	50
5.4. Exercises	52
Chapter 6. Completion and Dehn filling	55
6.1. Mostow–Prasad rigidity	55
6.2. Completion of incomplete structures on hyperbolic manifolds	55
6.3. Hyperbolic Dehn surgery space	59
6.4. Exercises	63
Bibliography	67
Index	69



## CHAPTER 1

# Introduction

### 1.1. Some motivation and history

Knots have been studied mathematically since approximately 1833, when Gauss developed the linking number of two knots. Peter Tait was one of the first to try to classify knots up to equivalence. He created the first knot tables, listing knots up to seven crossings [18]. However, the study of the geometry of knots, particularly hyperbolic geometry, did not really begin until the late 1970s and early 1980s, with work of William Thurston.

In the 1980s, William Thurston conjectured that every 3-manifold decomposes along spheres and incompressible tori into pieces that admit uniquely one of eight 3-dimensional geometries (geometric structures) [20]. This is the geometrization conjecture, and the proof of the full conjecture was announced in 2003 by Perelman. However, Thurston proved the conjecture for certain classes of manifolds, including manifolds with boundary, in the early 1980s. In fact, it has been known for nearly three decades that knot complements in  $S^3$  decompose into geometric pieces.

What are the eight 3-dimensional geometries? Peter Scott has written an excellent introduction to these geometries [17]. For our purposes, we need to know that six of the eight geometries are so-called *Seifert fibered*, and the last and most important geometry is hyperbolic.

Thurston showed that a knot complement will either be Seifert fibered, toroidal, meaning it contains an embedded incompressible torus, or hyperbolic. If the knot is toroidal, to obtain its geometric pieces one must cut along the incompressible torus and consider each resulting piece separately. We know exactly which knot complements are Seifert fibered, toroidal, or hyperbolic, again due to work of Thurston in the 1980s.

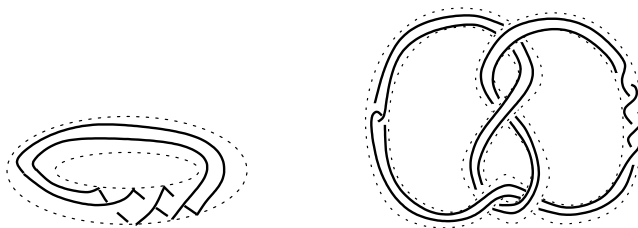


FIGURE 1.1. Left: a torus knot. Right: a satellite knot.

**THEOREM 1.1** (Thurston [20]). *The knots whose complement can be Seifert fibered consist of torus knots: knots which can be drawn on the surface of a torus, as in Figure 1.1. Toroidal knot complements are exactly the satellite knots: knots which can be drawn inside the complement of a (possibly knotted) solid torus, as on the right in Figure 1.1. All other knots are hyperbolic.*

Hyperbolic knots form the largest and least understood class of knots. Of all knots up to 16 crossings, classified by Hoste, Thistlethwaite, and Weeks [8], 13 are torus knots, 20 are satellite knots, and the remaining 1,701,903 are hyperbolic.

By the Mostow–Prasad rigidity theorem [13, 14], if a knot complement admits a hyperbolic structure, then that structure is unique. More carefully, Mostow showed that if there was an isomorphism between the fundamental groups of two closed hyperbolic 3–manifolds, then there was an isometry taking one to the other. Prasad extended this work to 3–manifolds with torus boundary, including knot complements. Thus if two hyperbolic knot complements have isomorphic fundamental group, then they have exactly the same hyperbolic structure. Finally, Gordon and Luecke showed that if two knot complements have the same fundamental group, then the knots are equivalent [5] (up to mirror reflection). Thus a hyperbolic structure on a knot complement is a complete invariant of the knot. If we could completely understand hyperbolic structures on knot complements, we could completely classify hyperbolic knots.

## 1.2. Basic terminology

**DEFINITION 1.2.** A *knot*  $K \subset S^3$  is a subset of points homeomorphic to a circle  $S^1$  under a piecewise linear (PL) homeomorphism. We may also think of a knot as a PL embedding  $K: S^1 \rightarrow S^3$ . We will use the same symbol  $K$  to refer to the map and its image  $K(S^1)$ .

More generally, a *link* is a subset of  $S^3$  PL homeomorphic to a disjoint union of copies of  $S^1$ . Alternately, we may think of a link as a PL embedding of a disjoint union of copies of  $S^1$  into  $S^3$ .

We assume our knots are piecewise linear to avoid wild knots. While wild knots may have interesting geometry, we won't be concerned with them in these notes.

**DEFINITION 1.3.** We will say that two knots (or links)  $K_1$  and  $K_2$  are equivalent if they are *ambient isotopic*, that is, if there is a (PL) homotopy  $h: S^3 \times [0, 1] \rightarrow S^3$  such that  $h(*, t) = h_t: S^3 \rightarrow S^3$  is a homeomorphism for each  $t$ , and  $h(K_1, 0) = h_0(K_1) = K_1$  and  $h(K_1, 1) = h_1(K_1) = K_2$ .

What we will deal with in this course is a special type of 3–manifold, the *knot complement* (or link complement).

**DEFINITION 1.4.** For a knot  $K$ , let  $N(K)$  denote an open regular neighborhood of  $K$  in  $S^3$ . The *knot complement* is the manifold  $S^3 \setminus N(K)$ .

Notice that it is a compact 3-manifold with boundary homeomorphic to a torus.

For our applications, we will typically be interested in the interior of the manifold  $S^3 \setminus N(K)$ . I will denote this manifold by  $S^3 \setminus K$ , and usually (somewhat sloppily) just refer to this manifold as the knot complement.

DEFINITION 1.5. A *knot invariant* (or link invariant) is a function from the set of links to some other set whose value depends only on the equivalence class of the link.

Knot and link invariants are used to prove that two knots or links are distinct, or to measure the complexity of the link in various ways.

We wish to put a hyperbolic structure on (the interior of) our knot complements. We will define a hyperbolic structure on a manifold more carefully during the course. For now, if a manifold has a hyperbolic structure, then we can measure geometric information about the manifold, including lengths of geodesics, volume, minimal surfaces, etc.



## CHAPTER 2

# Polyhedral decomposition of the Figure–8 knot complement

### 2.1. Introduction

We are going to decompose the figure-8 knot complement into ideal polyhedra. This decomposition appears in Thurston’s notes [19], and with a little more explanation in his book [21]. Menasco generalized the procedure to all link complements [12]. His work is essentially what we present below.

### 2.2. Vocabulary

DEFINITION 2.1. A *knot diagram* is a 4–valent graph with over/under crossing information at each vertex. Figure 2.1 shows a diagram of the Figure-8 knot complement.

DEFINITION 2.2. A *polyhedron* is a closed 3–ball whose boundary is labeled with a finite number of simply connected faces, edges, and vertices.

An *ideal polyhedron* is a 3–ball whose boundary is labeled with a finite number of simply connected faces, edges, and vertices, but all of whose vertices have been removed. That is, to form an ideal polyhedron, start with a regular polyhedron and remove the points corresponding to vertices.

### 2.3. Polyhedra

Sometimes it is easier to study manifolds if we split them into smaller, simpler pieces. We are interested in knot complements  $S^3 \setminus K$ . We will cut  $S^3 \setminus K$  into two ideal polyhedra. We will then have a description of  $S^3 \setminus K$  as a gluing of two ideal polyhedra. That is, given a description of the polyhedra, and gluing information on the faces of the polyhedra, we may reconstruct the knot complement  $S^3 \setminus K$ .

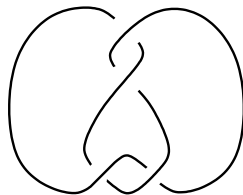


FIGURE 2.1. A diagram of the figure–8 knot

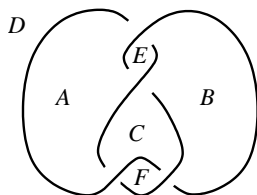
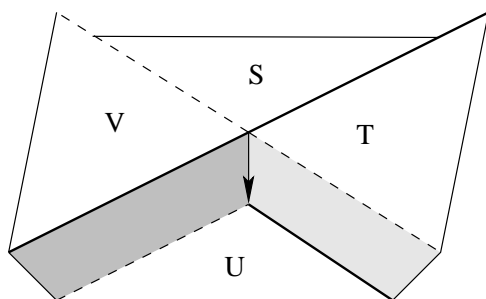


FIGURE 2.2. Faces for the figure-8 knot.

FIGURE 2.3. The knot is shown in bold. Faces labeled  $U$  and  $T$  meet at the edge shown.

The example we will walk through is that of the figure-8 knot complement. We will see that this particular knot complement has many nice properties.

As homework, you will be asked to walk through the techniques below to determine decompositions of other knot complements into ideal polyhedra.

**2.3.1. Overview.** Start with a diagram of the knot. There will be two polyhedra in our decomposition. These can be visualized as two balloons: One balloon expands above the diagram, and one balloon expands below the diagram. As the balloons continue expanding, they will bump into each other in the regions cut out by the graph of the diagram. Label these regions. In Figure 2.2, the regions are labeled  $A$ ,  $B$ ,  $C$ ,  $D$ ,  $E$ , and  $F$ . These will correspond to faces of the polyhedra.

The faces meet up in edges. There is one edge for each crossing. It runs vertically from the knot at the top of the crossing to the knot at the bottom (or the other way around). The balloon expands until faces meet at edges. Figure 2.3 shows how the top balloon would expand at a crossing. The edge is drawn as an arrow from the top of the crossing to the bottom. Faces labeled  $T$  and  $U$  meet across the edge. Rotating the picture  $180^\circ$  about the edge, we would see an identical picture with  $S$  meeting  $V$ .

It may be helpful to examine the meeting of faces at an edge by 3-dimensional model. Henry Segerman has come up with a paper model to illustrate the phenomenon of Figure 2.3. Start with a sheet of paper labeled as in Figure 2.4. Cut out the shaded square in the middle. Now

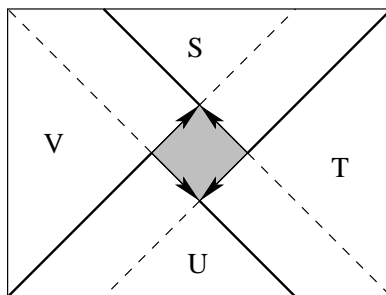


FIGURE 2.4. Cut out the shaded square. Start with a pair of parallel lines. Fold the bold part of the line in a direction opposite that of the dashed part of the line. Fold parallel bold and dashed lines in opposite directions. Correct folding results in a model that looks like Figure 2.3.

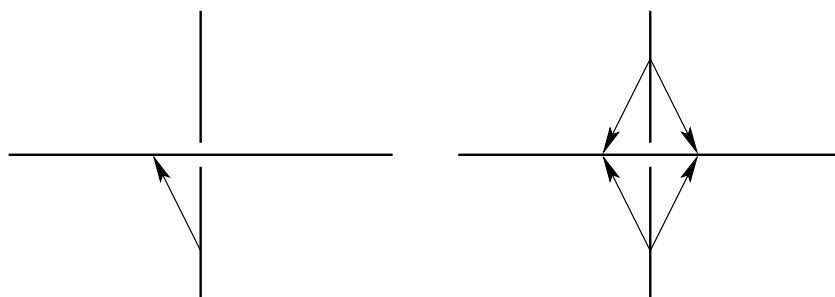


FIGURE 2.5. A single edge.

fold the paper until it looks like that in Figure 2.3. By rotating the paper model, we can see how faces meet up.

Stringing crossings such as this one together, we obtain the complete polyhedral decomposition of the knot. This is the geometric intuition behind the polyhedral expansion. We now explain a combinatorial method to describe the polyhedra.

### 2.3.2. Step 1. Sketch faces and edges into the diagram.

Recall a diagram is a 4-valent graph lying on a plane, the plane of projection. The regions of the plane of projection cut out by the graph will be the faces, including the outermost unbounded region of the plane of projection. We start by labeling those, in Figure 2.2.

Edges come from arcs that connect the two strands of the diagram at a crossing. For ease of explanation, we are going to draw each edge four times, as follows. Shown on the left of Figure 2.5 is a single edge corresponding to a crossing. Note that the edge is ambient isotopic in  $S^3$  to the three additional edges shown on the right in Figure 2.5.

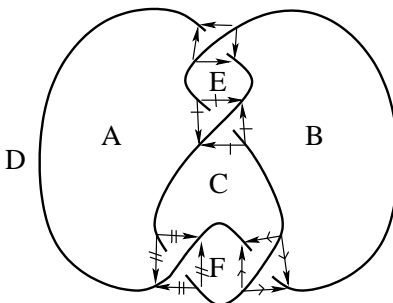


FIGURE 2.6. Edges of the figure-8 knot

The reason for sketching each edge four times is that it allows us to visualize easily which edges bound the faces we have already labeled. In Figure 2.6, we drew four copies of each of the four edges we get from crossings of the diagram. Note that the face labeled  $A$ , for example, will be bordered by three edges, one with two tick marks, one with a single tick mark, and one with no tick marks.

**2.3.3. Step 2.** Shrink the knot to ideal vertices on the top polyhedron.

Now we come to the reason for using *ideal* polyhedra, rather than regular polyhedra. Notice that the edges stretch from a part of the knot to a part of the knot. However, the manifold we are trying to model is the knot complement,  $S^3 \setminus K$ . Therefore, the knot  $K$  does not exist in the manifold. An edge with its two vertices on  $K$  must necessarily be an ideal edge, i.e. its vertices are not contained in the manifold  $S^3 \setminus K$ .

Since the knot is *not* part of the manifold, we will shrink strands of the knot to ideal vertices. Focus first on the polyhedron on top. Each component of the knot we “see” from inside the top polyhedron will be shrunk to a single ideal vertex. These visible knot components correspond to sequences of overcrossings of the diagram. Compare to Figure 2.3 — note that at an undercrossing, the component of the knot ends in an edge, but at an overcrossing the knot continues on. Moreover, note that at an undercrossing, the knot runs into just one edge, but at an overcrossing the knot passes the same edge twice, once on each side.

In terms of the four copies of the edge in Figure 2.5, when we consider the polyhedron on top, we may identify the two edges which are isotopic along an overstrand, but not those isotopic along understrands. See Figure 2.7.

Shrink each overstrand to a single ideal vertex. The result is pattern of faces, edges, and ideal vertices for the top polyhedron, shown in Figure 2.8. Notice that the face  $D$  is a disk, containing the point at infinity.

**2.3.4. Step 3.** Shrink the knot to ideal vertices for the bottom polyhedron.

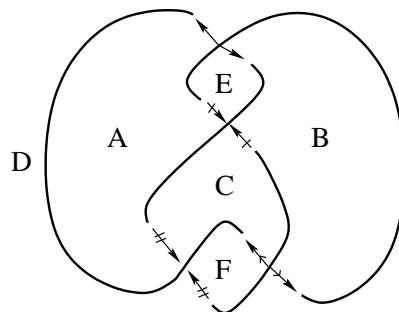


FIGURE 2.7. Isotopic edges in top polyhedron identified.

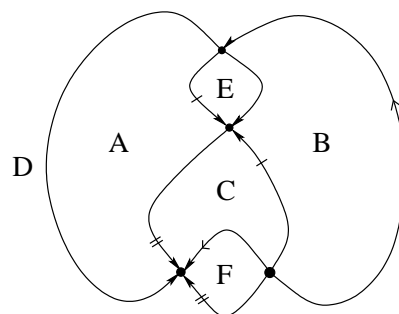


FIGURE 2.8. Top polyhedron, viewed from the inside.

Notice that underneath the knot, the picture of faces, edges, and vertices will be slightly different. In particular, when finding the top polyhedron, we collapsed overstrands to a single ideal vertex. When you put your head underneath the knot, what appear as overstrands from below will appear as understrands on the usual knot diagram.

The easiest way to see this difference is to take the 3-dimensional model constructed in Figure 2.4. Figure 2.3 shows the view of the faces meeting at an edge from the top. If you turn the model over to the opposite side, you will see how the faces meet underneath. Figure 2.9 illustrates this. Note  $U$  now meets  $T$ , and  $S$  meets  $V$ .

In terms of the combinatorics, edges of Figure 2.5 which are isotopic by sliding an endpoint along an understrand are identified to each other on the bottom polyhedron, but edges only isotopic by sliding an endpoint along an overstrand are not identified.

As above, collapse each knot strand corresponding to an understrand to a single ideal vertex. The result is Figure 2.10.

One thing to notice: we sketched the top polyhedron with our heads inside the ball on top, looking out. If we move the face  $D$  away from the point at infinity, then it wraps *above* the other faces shown in Figure 2.8.

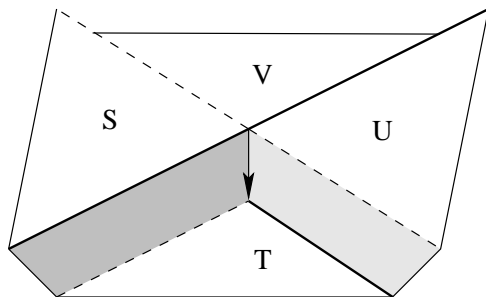


FIGURE 2.9. 3-dimensional model, opposite side as in Figure 2.3.

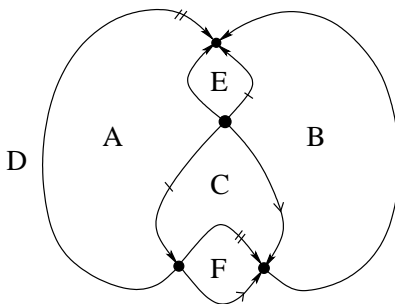


FIGURE 2.10. Bottom polyhedron, viewed from the outside.

On the other hand, we sketched the bottom polyhedron with our heads outside the ball on the bottom. If we move the face  $D$  away from the point at infinity, it wraps *below* the other faces shown in Figure 2.10.

#### 2.4. Exercises

This polyhedral decomposition works for any knot or link diagram, to give a polyhedral decomposition of its complement.

**EXERCISE 2.1.** As a warmup exercise, determine the polyhedral decomposition for one (or more) of the knots shown in Figure 2.11. Sketch both top and bottom polyhedra.

**DEFINITION 2.3.** An *alternating* diagram is one in which crossings alternate between over and under as we travel along the diagram in a fixed direction.

All the examples of knot diagrams we have encountered so far are alternating. The diagram of the knot  $8_{19}$  in Figure 2.12 is not alternating. (In fact, the knot  $8_{19}$  has no alternating diagram.)

**EXERCISE 2.2.** Determine the polyhedral decomposition for the given diagram of the knot  $8_{19}$ . Note: as above, many ideal vertices are obtained

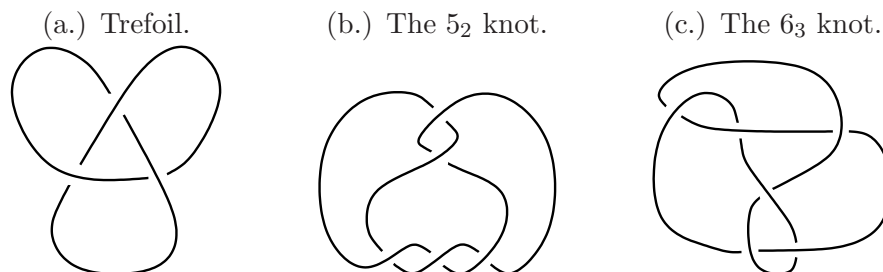
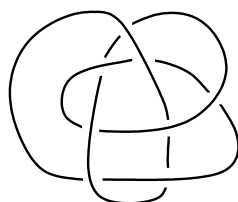


FIGURE 2.11. Three examples of knots.

FIGURE 2.12. The knot  $8_{19}$ , which has no alternating diagram.

by shrinking overstrands to a point. However, you will have to use, for example, Figure 2.3 to determine what happens between two understrands.

- EXERCISE 2.3.            (a) If a knot diagram is alternating, we obtain a very special ideal polyhedron. In particular, all ideal vertices will have the same valence. What is it? Show that the ideal vertices for an alternating knot all have this valence.
- (b) What are the possible valences of ideal vertices in general (i.e. for non-alternating knots)? For which  $n \geq 0 \in \mathbb{Z}$  is there a knot diagram whose polyhedral decomposition yields an ideal vertex of valence  $n$ ? Explain your answer, with (portions of) knot diagrams.

EXERCISE 2.4. Note that in the polyhedral decomposition for alternating knots, the polyhedra are given by simply labeling each ball with the projection graph of the knot and declaring each vertex to be ideal. Prove this statement for any alternating knot. Show the result is false for non-alternating knots.

EXERCISE 2.5. The decomposition admits a checkerboard coloring: faces are either white or shaded, and white faces meet shaded faces across an edge. Moreover, faces are identified from top to bottom by a “gear rotation”: white faces on the top are rotated once counter-clockwise and then glued to the identical face on the bottom; shaded faces are rotated once clockwise and then glued to the identical face on the bottom. This is shown for the figure-8 knot in Figure 2.13. Prove the above statement for any alternating knot.

The diagrams we have encountered so far are all reduced. We can follow the above procedure for non-reduced diagrams. For example, we obtain a

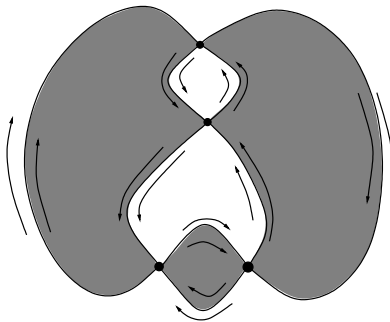


FIGURE 2.13. Checkerboard coloring and “gear rotation” for the figure-8 knot.

polyhedral decomposition for diagrams which contain *nugatory crossings*, as in Figure 2.14.



FIGURE 2.14. A nugatory crossing.

EXERCISE 2.6. Show that the polyhedral decomposition will contain a monogon, i.e. a face whose boundary is a single edge and a single vertex, if and only if the diagram has a nugatory crossing.

*Let bigons be bygone.* — William Menasco

DEFINITION 2.4. A *bigon* is a face of the polyhedral decomposition which has just two edges (and two ideal vertices).

Note that the two edges of a bigon face must be isotopic to each other. Hence, we sometimes will remove bigon faces from the polyhedral decomposition, identifying their two edges.

EXERCISE 2.7. For the figure-8 knot, sketch the two polyhedra we get when bigon faces are removed. How many edges are there in this new, bigon-free decomposition? The resulting polyhedra are well known solids in this case. What are they?

For each of the polyhedra obtained in exercise 1, sketch the resulting polyhedra with bigons removed.

EXERCISE 2.8. Suppose we start with any alternating knot, and do the polyhedral decomposition above, collapsing bigons at the last step. What are possible valences of vertices? Sketch the diagram of a single alternating knot that has all possible valences of ideal vertices in its polyhedral decomposition.

What valences of vertices can you get if you don't require the diagram to be alternating but collapse bigons? Can you find 1-valent vertices? For any  $n > 4 \in \mathbb{Z}$ , can you find  $n$ -valent vertices?



## CHAPTER 3

# Hyperbolic geometry and ideal tetrahedra

### 3.1. Basic hyperbolic geometry

Some good references for hyperbolic geometry are books by Anderson [2], Marden [11], Ratcliffe [15], and Thurston [21]. Here we include only some of the most basic information, and most importantly, exercises to help you get warmed up. For details and proofs of the following, we refer you to one of the previous references.

**3.1.1. 2–dimensional hyperbolic geometry.** We start with hyperbolic 2–space,  $\mathbb{H}^2$ , since it gives a nice warm up to hyperbolic 3–space,  $\mathbb{H}^3$ .

Define hyperbolic 2–space,  $\mathbb{H}^2$  as follows:

$$\mathbb{H}^2 = \{z = x + iy \in \mathbb{C} \mid y > 0\},$$

equipped with the metric

$$ds^2 = \frac{dx^2 + dy^2}{y^2}.$$

The geodesics in  $\mathbb{H}^2$  (i.e. distance minimizing lines) are exactly those lines and circles which meet the boundary  $\mathbb{R} \cup \{\infty\} = \{x + iy \mid y = 0\}$  of  $\mathbb{H}^2$  at right angles. That is, geodesics consist of vertical straight lines, which meet the real line in  $\mathbb{C}$  at a right angle, and semi-circles with center on the real line. See Figure 3.1.

Recall that an isometry preserves the metric, therefore preserves path lengths, areas, etc. The group of isometries of  $\mathbb{H}^2$  is generated by inversions of the upper half plane in hyperbolic geodesics. The group of orientation preserving isometries is the group  $\mathrm{PSL}(2, \mathbb{R})$ , acting as linear fractional

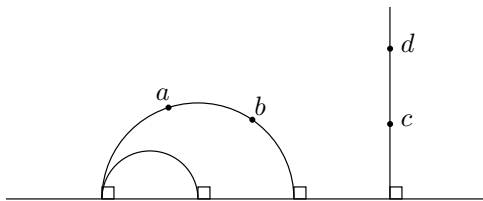


FIGURE 3.1. Some geodesics and points in  $\mathbb{H}^2$ .

transformations. That is, if  $A \in \text{PSL}(2, \mathbb{R})$  is given by

$$A = \begin{pmatrix} a & b \\ c & d \end{pmatrix},$$

where  $ad - bc = 1$ , then  $Az \in \mathbb{C}$  is given by

$$Az = \frac{az + b}{cz + d}.$$

Recall that linear fractional transformations take circles to circles and lines to lines.

Given any three points  $z_1, z_2$ , and  $z_3$  in  $\partial\mathbb{H}^2$ , there exists an isometry of  $\mathbb{H}^2$  taking  $z_1$  to 1,  $z_2$  to 0, and  $z_3$  to  $\infty$  (exercise). It follows that there exists an isometry of  $\mathbb{H}^2$  taking any three distinct points on  $\partial\mathbb{H}^2$  to any other three distinct points.

EXAMPLE 3.1. Length computation.

Suppose you wish to compute the length of a segment, or the distance between two points in  $\mathbb{H}^3$ . One strategy for computing is to apply an isometry taking the two points to a simpler picture. For example, in Figure 3.1, find an isometry taking  $a$  and  $b$  to  $c$  and  $d$ , respectively, where we assume the real coordinate of  $c$  and  $d$  is 0. In fact, we may assume  $c$  is the point  $0 + i \in \mathbb{C}$  and  $d$  is some point  $0 + ti$ .

Now one way to compute the distance between  $0 + i$  and  $0 + ti$  is to find the length of the path  $\gamma(s) = (0 + si)$  from  $s = 1$  to  $s = t$ . This can be computed by integration as in a calculus class, only now we integrate using the hyperbolic metric.

$$\begin{aligned} \text{Dist}(a, b) &= \int_1^t \|\gamma'(s)\|_{\text{hyp}} ds \\ &= \int_1^t \|\gamma'(s)\|_{\text{Eucl}} \frac{1}{s} ds \\ &= \int_1^t \frac{1}{s} ds \\ &= \log(t) \end{aligned}$$

DEFINITION 3.2. An *ideal triangle* in  $\mathbb{H}^2$  is a triangle with three geodesic edges, with all three vertices on  $\partial\mathbb{H}^2$ .

There is an isometry of  $\mathbb{H}^2$  taking any ideal triangle to the ideal triangle with vertices 0, 1, and  $\infty$ . Hence all ideal triangles in  $\mathbb{H}^2$  are isometric, so they have exactly the same area.

DEFINITION 3.3. A *horocycle* at an ideal point  $p \in \partial\mathbb{H}^2$  is defined as a curve perpendicular to all geodesics through  $p$ . When  $p$  is a point on  $\mathbb{R} \subset \partial\mathbb{H}^2 = \mathbb{R} \cup \{\infty\}$ , a horocycle is a Euclidean circle tangent to  $p$ , as in Figure 3.2. When  $p$  is the point  $\infty$ , a horocycle at  $p$  is a line parallel to  $\mathbb{R}$ .

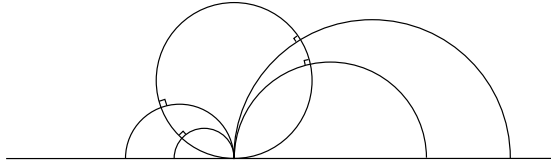


FIGURE 3.2. A horocycle

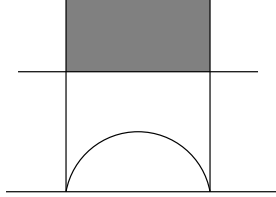


FIGURE 3.3. The region of example 3.5.

That is, in this case the horocycle consists of points of the form  $\{x + ic\}$  where  $c > 0$  is constant.

DEFINITION 3.4. A *horoball* is the region of  $\mathbb{H}^2$  interior to a horocycle.

Note a horoball will either be a Euclidean disk tangent to  $\mathbb{R} \subset \partial\mathbb{H}^2$  or a region consisting of points of the form  $\{x + ic \mid y > c\}$ .

EXAMPLE 3.5. Area of a region in  $\mathbb{H}^2$ .

In this example, we will compute the area of the region of  $\mathbb{H}^2$  bounded by the lines  $x = 0$ ,  $x = 1$ , and the horocycle  $y = 1$ . This region is shown in Figure 3.3.

As in a standard Euclidean multivariable calculus class, to find the area we can compute a double integral over the region  $0 \leq x \leq 1$  and  $y \geq 1$ . We use the hyperbolic area element, however:  $\frac{1}{y^2} dx dy$ .

$$\text{Area}(R) = \int_0^1 \int_1^\infty \frac{1}{y^2} dy dx = \int_0^1 1 dx = 1.$$

**3.1.2. 3-dimensional hyperbolic geometry.** Hyperbolic 3-space is defined as follows:

$$\mathbb{H}^3 = \{(x + iy, t) \in \mathbb{C} \times \mathbb{R} \mid t > 0\},$$

under the metric

$$ds^2 = \frac{dx^2 + dy^2 + dt^2}{t^2}.$$

Geodesics are again vertical lines and semicircles orthogonal to the boundary  $\partial\mathbb{H}^3 = \mathbb{C} \cup \{\infty\}$ . Totally geodesic planes are vertical planes and hemispheres centered on  $\mathbb{C}$ . The full group of isometries of  $\mathbb{H}^3$  is generated by inversions in these hemispheres. We often restrict to the subgroup of orientation preserving isometries. This group is  $\text{PSL}(2, \mathbb{C})$ . Its action on the

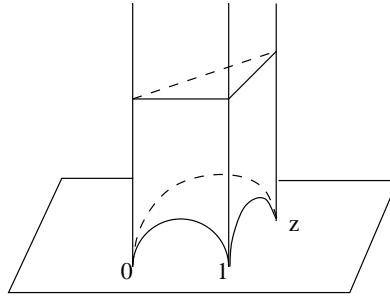


FIGURE 3.4. Ideal tetrahedron

boundary  $\partial\mathbb{H}^3 = \mathbb{C} \cup \{\infty\}$  is the usual action of  $\mathrm{PSL}(2, \mathbb{C})$  on  $\mathbb{C} \cup \{\infty\}$ . This action is extended to the upper half space. (Marden [11, Chapter 1] gives an excellent presentation of this.)

Recall that elements of  $\mathrm{PSL}(2, \mathbb{C})$  can be classified as one of three types: elliptic, which have two complex conjugate eigenvalues and a single fixed point in  $\mathbb{H}^2$ ; parabolic, which have one eigenvalue and one fixed point on the boundary  $\mathbb{R} \cup \{\infty\} = \partial\mathbb{H}^2$ ; and hyperbolic, which have two eigenvalues and two fixed points on  $\partial\mathbb{H}^2$ .

**DEFINITION 3.6.** An *ideal tetrahedron* is a tetrahedron in  $\mathbb{H}^3$  with all four vertices on  $\partial\mathbb{H}^3$ .

Since there exists a Möbius transformation taking any three points to 1, 0, and  $\infty$  in  $\mathbb{C} \cup \{\infty\}$ , we may assume our tetrahedron has vertices at 0, 1 and  $\infty$ , and at some point  $z \in \mathbb{C} \setminus \{0, 1\}$ . So any ideal tetrahedron is parameterized by  $z$ . See Figure 3.4.

Notice the argument of  $z$  is the dihedral angle between vertical planes through 0, 1,  $\infty$  and through 0,  $z$ ,  $\infty$ . Take the hyperbolic geodesic through  $z \in \mathbb{C}$  that meets the vertical line from 0 to  $\infty$  in a right angle. Take another geodesic through  $1 \in \mathbb{C}$  that meets the vertical line from 0 to  $\infty$  at a right angle. The hyperbolic distance between the endpoints of the perpendiculars on the line from 0 to  $\infty$  is  $|\ln |z||$  (exercise). Hence

$$\ln z = (\text{signed dist between altitudes}) + i(\text{dihedral angle}).$$

**DEFINITION 3.7.** A *horosphere* about  $\infty$  in  $\partial\mathbb{H}^3$  is a plane parallel to  $\mathbb{C}$ , consisting of points  $\{(x + iy, c) \in \mathbb{C} \times \mathbb{R}\}$  where  $c > 0$  is constant. Note for any  $c > 0$ , it is perpendicular to all geodesics through  $\infty$ . When we apply an isometry that takes  $\infty$  to some  $p \in \mathbb{C}$ , a horosphere is taken to a Euclidean sphere tangent to  $p$ . By definition, this is a horosphere about  $p$ . A *horoball* is the region interior to a horosphere.

The induced metric on a horosphere is Euclidean. When we intersect horospheres about 0, 1,  $\infty$  and  $z$  with an ideal tetrahedron through those points, we get four Euclidean triangles. These four triangles are similar (exercise).

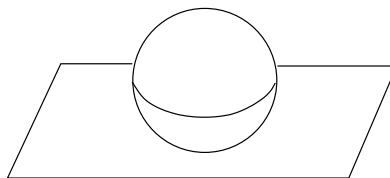


FIGURE 3.5. Horosphere

### 3.2. Exercises

EXERCISE 3.1. Work through the classification of isometries of  $\mathbb{H}^2$  as elliptic, parabolic, or hyperbolic. (Thurston, page 67 [19]).

EXERCISE 3.2. Isometries.

- Given any three points  $b$ ,  $c$  and  $d$  in  $\partial\mathbb{H}^2$ , prove that there exists an isometry of  $\mathbb{H}^2$  taking  $b$  to 1,  $c$  to 0, and  $d$  to  $\infty$ . What is it? When will it be orientation preserving? If it happens to be orientation preserving, write it as an element of  $\mathrm{PSL}(2, \mathbb{R})$ .
- Similarly, given  $b$ ,  $c$  and  $d$  in  $\mathbb{C} \cup \{\infty\}$ , prove there exists an orientation preserving isometry of  $\mathbb{H}^3$  taking  $b$  to 1,  $c$  to 0, and  $d$  to  $\infty$ . Write it down as a matrix in  $\mathrm{PSL}(2, \mathbb{C})$ .

EXERCISE 3.3. Cross ratios.

Given  $a \in \mathbb{C}$ , the image of  $a$  under the isometry of exercise (2)(b) is the *cross ratio* of  $a, b, c, d$ , and is denoted  $\lambda(a, b; c, d)$ .

Let  $x$  be the point on the geodesic in  $\mathbb{H}^3$  between  $c$  and  $d$  such that the geodesic from  $a$  to  $x$  is perpendicular to that between  $c$  and  $d$ . Let  $y$  be the point on the geodesic between  $c$  and  $d$  such that the geodesic from  $b$  to  $y$  is perpendicular to that between  $c$  and  $d$ . Prove the hyperbolic distance between  $x$  and  $y$  is equal to  $|\ln |\lambda(a, b; c, d)||$ .

EXERCISE 3.4. Areas of ideal triangles.

Prove that the area of an ideal hyperbolic triangle is  $\pi$ . (E.g. use calculus.)

EXERCISE 3.5. Areas of 2/3-ideal triangles.

- A 2/3-ideal triangle is a triangle with two vertices at infinity, and the third in the interior of  $\mathbb{H}^2$  such that the interior angle at the third vertex is  $\theta$ . Show that all 2/3-ideal triangles of angle  $\theta$  are congruent to the triangle shown in Figure 3.6.
- Define a function  $A: (0, \pi) \rightarrow \mathbb{R}$  by:  $A(\theta)$  is the area of the 2/3-ideal triangle with interior angle  $\pi - \theta$ . Show that  $A(\theta_1 + \theta_2) = A(\theta_1) + A(\theta_2)$ . (Hint: Figure 3.7 may be useful.)
- It follows that  $A$  is  $\mathbb{Q}$ -linear. Since  $A$  is continuous, it must be  $\mathbb{R}$ -linear. Show  $A(\theta) = \theta$ .

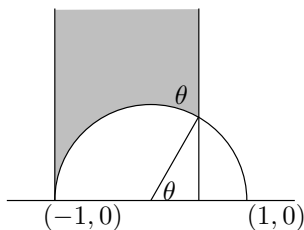
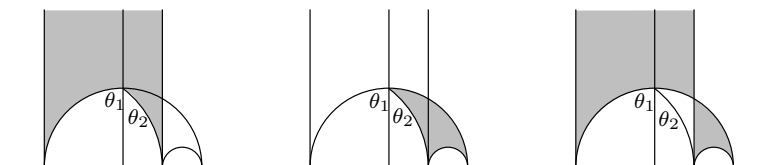
FIGURE 3.6.  $2/3$ -ideal triangle.

FIGURE 3.7. Areas of triangles.

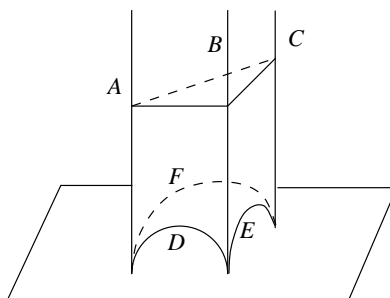


FIGURE 3.8.

EXERCISE 3.6. Areas of general triangles.

Using the previous two problems, show that the area of a triangle with interior angles  $\alpha$ ,  $\beta$ , and  $\gamma$  is equal to  $\pi - \alpha - \beta - \gamma$ . Note an ideal vertex has interior angle 0.

EXERCISE 3.7. Ideal tetrahedra and dihedral angles.

- The dihedral angles on a tetrahedron are labeled  $A$ ,  $B$ ,  $C$ ,  $D$ ,  $E$ , and  $F$  in Figure 3.8. Using linear algebra, prove that opposite dihedral angles agree. That is, show  $A = E$ ,  $B = F$ , and  $C = D$ .
- Prove the same thing using Möbius transformations: If the ideal tetrahedron has ideal vertices at  $0$ ,  $1$ ,  $\infty$ , and  $z$ , show that the triangles cut off by horospheres are similar by applying isometries, taking each ideal vertex to infinity carefully, and comparing the results.

EXERCISE 3.8. Ideal tetrahedra and cross ratios. Orient an ideal tetrahedron with vertices  $a, b, c, d$ . When we apply a Möbius transformation taking  $b, c, d$  to  $1, 0, \infty$ , respectively, the point  $a$  goes to the cross ratio  $\lambda(a, b; c, d)$ .

Label the edge from  $c$  to  $d$  by the complex number  $\lambda = \lambda(a, b; c, d)$ . We may do this for each edge of the tetrahedron, labeling by a different cross ratio. (Notice you need to keep track of orientation.) Find all labels on the edges of the tetrahedra in terms of  $\lambda$ .

EXERCISE 3.9. Symmetries. The group of symmetries of a generic hyperbolic ideal tetrahedron is isomorphic to  $\mathbb{Z}_2 \times \mathbb{Z}_2$ . For each of the three nontrivial elements of  $\mathbb{Z}_2 \times \mathbb{Z}_2$ , find a symmetry of the ideal tetrahedron corresponding to that element. Describe the symmetry geometrically.



## CHAPTER 4

### Geometric structures on manifolds

In the first chapter, we discussed decomposing manifolds into topological ideal polyhedra. In the second chapter, we discussed basic hyperbolic geometry, including hyperbolic structures on ideal tetrahedra. In this chapter, we will begin to put these together and discuss hyperbolic structures on manifolds.

**Note:** In this section, we lean very heavily on Chapter 3 of Thurston [21], particularly sections 3.1 through 3.4. Our focus and exposition differs slightly, but you may want to read that book to help you understand these notes. Or the other way around.

#### 4.1. Geometric structures

**4.1.1. Introductory example: The torus.** A geometric structure you are familiar with is a 2-dimensional Euclidean structure on a torus. Choose your favorite parallelogram. Obtain the torus by gluing the top and bottom of the parallelogram, as well as the two sides, in an orientation preserving manner.

Alternately, construct the universal cover of the torus by gluing copies of the parallelogram to form a tiling of the plane, as in Figure 4.1.

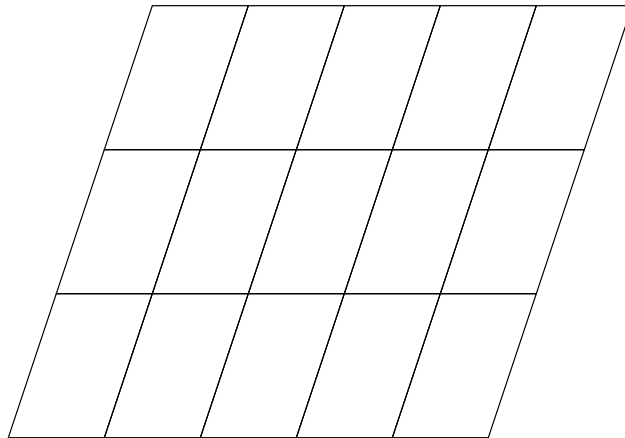


FIGURE 4.1. The universal cover of a Euclidean torus.

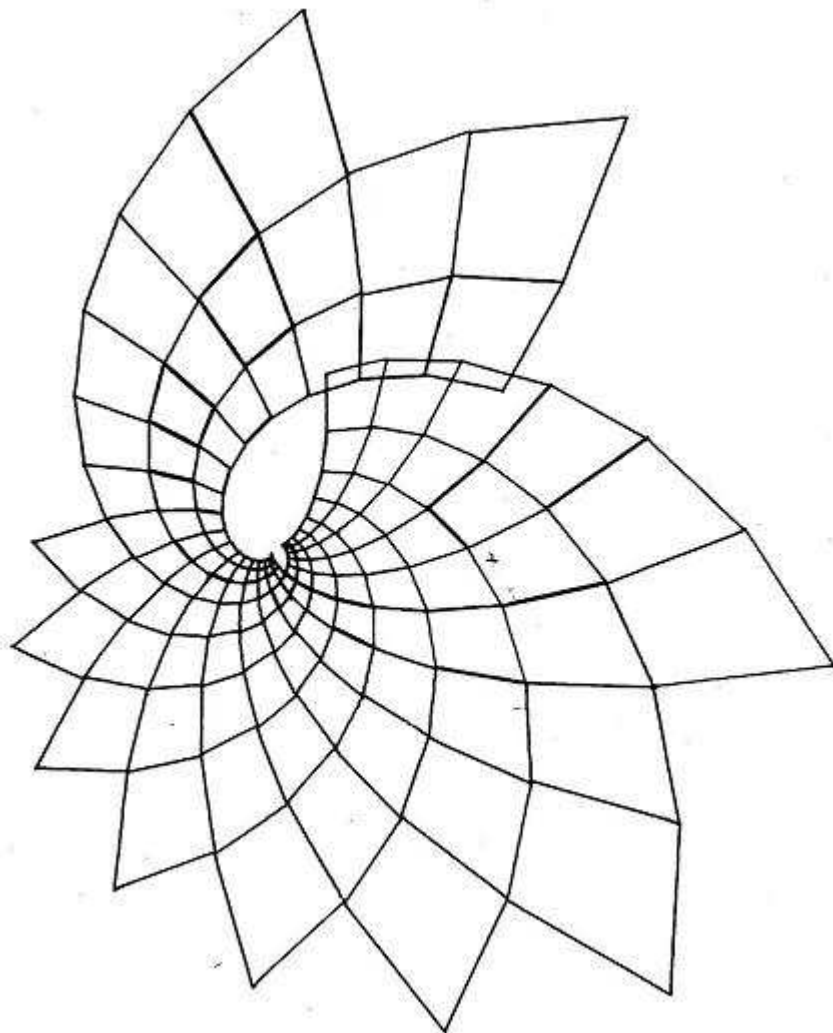


FIGURE 4.2. When we construct a torus from a quadrilateral, generally a single point is omitted from the plane. (This is a copy of a figure from [19].)

Modify this construction by choosing a more general quadrilateral instead of a parallelogram. We can still identify opposite sides in an orientation preserving manner, so when we glue we still get a topological torus. However, when we glue copies of the quadrilateral to itself, as we did when constructing the universal cover above, we have to shrink, expand, and rotate the quadrilateral to glue copies, and the result is not a tiling of the plane. See Figure 4.2.

The torus was created by gluing quadrilaterals. More generally, we will glue different types of polygons, including ideal polygons, and in 3-dimensions, polyhedra.

DEFINITION 4.1. Let  $M$  be a 2-manifold. A *topological polygonal decomposition* of  $M$  is a combinatorial way of gluing polygons so that the result is homeomorphic to  $M$ .

Notes:

- We allow ideal polygons, i.e. those with one or more ideal vertex.
- By *gluing* we mean something simplicial. That is, distinct polygons meet only at an edge of both, and distinct edges meet only at a vertex of both.

Both constructions of the torus above give examples.

DEFINITION 4.2. A *geometric polygonal decomposition* of  $M$  is a topological polygonal decomposition along with a metric on each polygon such that gluing is by isometry and the result of the gluing is a smooth manifold with a complete metric.

The second construction of the torus is incomplete: We may take a Cauchy sequence of points in the plane converging to the omitted point in Figure 4.2. These project to give a Cauchy sequence in the torus that does not converge. Hence this example does not give a geometric polygonal decomposition.

We will be studying polygonal decompositions of manifolds and their generalization to three dimensions: polyhedral decompositions. More generally, we can discuss geometric structures on manifolds.

#### 4.1.2. Geometric structures on manifolds.

DEFINITION 4.3. Let  $X$  be a manifold, and  $G$  a group acting on  $X$ . We say a manifold  $M$  has a  $(G, X)$ -structure if for every point  $x \in M$ , there exists a *chart*  $(U, \phi)$ , that is, a neighborhood  $U \subset M$  of  $x$  and a homeomorphism  $\phi: U \rightarrow X$ . Charts satisfy the following: If two charts  $(U, \phi)$  and  $(V, \psi)$  overlap, then the *transition map* or *coordinate change*

$$\gamma = \phi \circ \psi^{-1}: \psi(U \cap V) \rightarrow \phi(U \cap V)$$

is an element of  $G$ .

We will take  $X$  to be simply connected, and  $G$  a group of real analytic diffeomorphisms acting transitively on  $X$ . Recall that real analytic diffeomorphisms are uniquely determined by their restriction to any open set. This is true, for example, of isometries of Euclidean space, and isometries of hyperbolic space.

EXAMPLE 4.4 (The Euclidean torus). Let  $X$  be 2-dimensional Euclidean space,  $\mathbb{E}^2$ . Let  $G$  be isometries of Euclidean space,  $\text{Isom}(\mathbb{E}^2)$ . The torus admits a  $(\text{Isom}(\mathbb{E}^2), \mathbb{E}^2)$  structure, also called a *Euclidean structure*.

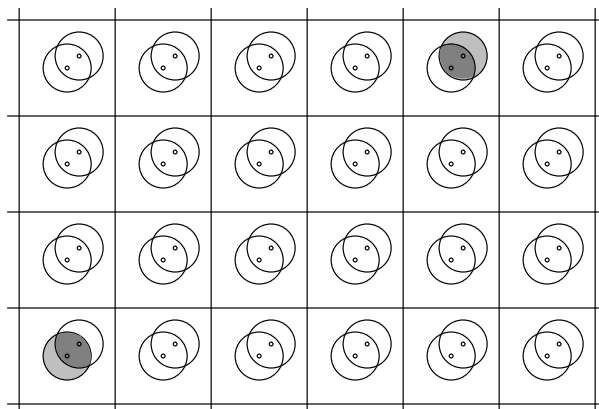


FIGURE 4.3. Euclidean structure on a torus: Transition maps are Euclidean translations.

To help us understand the definition, let's look at some charts and overlap maps for this example.

We know the universal cover of the torus is given by tiling the plane  $\mathbb{R}^2$  with parallelogram. Pick your favorite such tiling. My favorite tiling is the one where each parallelogram is a unit square, with one square with vertices at  $(0,0)$ ,  $(1,0)$ ,  $(1,1)$ , and  $(0,1)$  in  $\mathbb{R}^2$ . Now pick any point  $p$  on the torus. This will lift to a collection of points on  $\mathbb{R}^2$ , one for each copy of the unit square. Take a disk of radius  $1/4$ , say, around each lift. These all project under the covering map to an open neighborhood  $U$  of  $p$  in the torus. Therefore we have the following charts:  $(U, \phi)$  is a chart, where  $\phi$  maps  $U$  into the disk of radius  $1/4$  centered around the lift of  $p$  in the unit square with corners  $(0,0)$ ,  $(1,0)$ , and  $(0,1)$ . Another chart is  $(U, \psi)$ , where  $\psi$  maps  $U$  into the disk of radius  $1/4$  about the lift of  $p$  in some other square. No matter which other square  $\psi$  maps into,  $\phi \circ \psi^{-1}$  will be a Euclidean translation by integral values in the  $x$  and  $y$  direction. These are Euclidean isometries.

More generally, let  $q$  be a point such that the distance between a lift of  $q$  to our tiling of  $\mathbb{R}^2$  by unit squares is less than  $1/2$  from a lift of  $p$ . Thus a disk of radius  $1/4$  about this lift of  $p$  overlaps with a disk of radius  $1/4$  about the lift of  $q$ . These disks both project to give open neighborhoods  $U$  and  $V$  of  $p$  and  $q$  respectively in the torus. Since these neighborhoods overlap, we need to ensure that the corresponding charts differ by a Euclidean isometry in the region of overlap. Obtain charts by mapping  $U$  to your favorite disk of radius  $1/4$  about a lift of  $p$ . Map  $V$  to your favorite disk of radius  $1/4$  about a lift of  $q$  in  $\mathbb{R}^2$ . Again, regardless of the choice of  $\phi$  and  $\psi$ , the overlap  $\phi \circ \psi^{-1}$  will be a Euclidean translation by some integer amount in  $x$  and  $y$  directions.

Therefore, we conclude that the charts obtained by reading disks of radius  $1/4$  off of the universal cover of the torus give a Euclidean structure on the torus.

EXAMPLE 4.5 (The affine torus). Again let  $X = \mathbb{E}^2$ , but this time let  $G$  be the affine group acting on  $\mathbb{R}^2$ . That is,  $G$  consists of invertible affine transformations, where recall an affine transformation is a linear transformation followed by a translation:

$$x \mapsto Ax + b.$$

The torus of Figure 4.2 admits a  $(G, \mathbb{E}^2)$  structure. This can be seen in a manner similar to that in the previous example. Charts will differ by a scaling, rotation, then translation.

In practice, we rarely use charts to show manifolds have a particular  $(G, X)$ -structure. Instead, we build manifolds by starting with an existing manifold and quotienting out by the action of a group, or by gluing together polygons.

**4.1.3. Hyperbolic surfaces.** Let  $X = \mathbb{H}^2$ , and let  $G = \text{Isom}(\mathbb{H}^2)$ , the group of isometries of  $\mathbb{H}^2$ . When a 2-manifold admits an  $(\text{Isom}(\mathbb{H}^2), \mathbb{H}^2)$ -structure, we say the manifold admits a *hyperbolic structure*, or is hyperbolic.

We will look at some examples of hyperbolic 2-manifolds obtained from geometric polygonal decompositions. To do so, we start with a collection of hyperbolic polygons in  $\mathbb{H}^2$ , for example, a collection of triangles. We will assume each polygon is convex, and edges are portions of geodesics in  $\mathbb{H}^2$ . To each edge, associate exactly one other edge. Glue polygons along associated edges.

When does the result of this gluing admit a hyperbolic structure? We obtain a hyperbolic structure exactly when each point in the result has a neighborhood  $U$  and a homeomorphism into  $\mathbb{H}^2$  so that overlap maps are in  $\text{Isom}(\mathbb{H}^2)$ . This is equivalent to showing that each point has a neighborhood isometric to a disk in the hyperbolic plane (exercise 4.3).

When does each point in a gluing of hyperbolic polygons have a neighborhood isometric to a disk in the hyperbolic plane? Let  $x$  be a point in one of the polygons.

- (1) If  $x$  is in the interior of a polygon, then it has a neighborhood isometric to a ball in  $\mathbb{H}^2$ . (Duh.)
- (2) If  $x$  is on an edge of a polygon, then it has a neighborhood isometric to a “half-ball”. It is glued to exactly one point on some other edge of a polygon, which also has a “half-ball” neighborhood. These patch up correctly to give a neighborhood isometric to a ball.
- (3) If  $x$  is a finite vertex of a polygon, then we need to be careful.

CLAIM 4.6. *A gluing of hyperbolic polygons gives a manifold with a hyperbolic structure if and only if for each vertex, the angle sum is  $2\pi$ .*

PROOF. Exercise. □

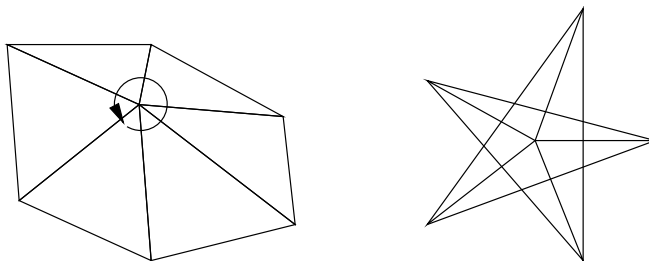


FIGURE 4.4. Non-singular structure if and only if angle sum around each vertex is  $2\pi$ .

## 4.2. Complete structures

Given a gluing of hyperbolic polygons, suppose the angle sum at each vertex is  $2\pi$ . Does it necessarily follow that we have a geometric polygonal decomposition (Definition 4.2)?

Recall that for a geometric polygonal decomposition, we needed a geometric structure on each polygon so that the result of the gluing is a smooth manifold with a complete metric. We have a smooth manifold with a metric. However, in the presence of ideal vertices, the metric may not be complete.

It will be easier to discuss criteria for completeness using the language of *developing maps* and *holonomy*.

**4.2.1. Developing maps and holonomy.** Developing maps and holonomy are described very well in Thurston's book, [21, pages 139–141]. At this point in my course, I distributed these three pages to students, which was perfectly fine to do using US fair use copyright laws. Unfortunately, to make these notes complete and self contained, I will need to reproduce some of that discussion. Hence the notation and exposition from here to Example 4.10 is very similar to that in [21].

We now restrict to the case that  $X$  is a real analytic manifold, and  $G$  is a group of real analytic diffeomorphisms acting transitively on  $X$ . For example, hyperbolic space and its isometries are real analytic, as is Euclidean space with its isometries. The key feature of real analytic manifolds that we need is that any element of  $G$  is completely determined by its restriction to an open subset of  $X$ .

Now, let  $M$  be a  $(G, X)$ -manifold, and let  $(U_1, \phi_1), (U_2, \phi_2), \dots$  be charts for  $M$ , with transition functions

$$\gamma_{ij} = \phi_i \circ \phi_j^{-1}.$$

By definition, each  $\gamma_{ij}$  agrees with an element of  $G$  on  $\phi_j(U_i \cap U_j)$ . Composing with  $\phi_j^{-1}$ , we get a locally constant map from  $U_i \cap U_j$  into  $G$ , which we will also call  $\gamma_{ij}$ .

Suppose both  $U_i$  and  $U_j$  contain  $x$ . Then note that the maps  $\phi_i: U_i \rightarrow X$  and  $\gamma_{ij}(x)\phi_j: U_j \rightarrow X$  agree on the component of  $U_i \cap U_j$  that contains  $x$ , and so we can view  $\gamma_{ij}(x)\phi_j$  as extending  $\phi_i$ . We will generally run into

inconsistencies if we try to extend  $\phi_i$  too far. To fix this, we look at the universal cover of  $M$ .

Recall that the universal cover  $\widetilde{M}$  of  $M$  is defined to be the space of homotopy classes of paths in  $M$  that start at a fixed basepoint  $x_0$ . Take a path  $\alpha: [0, 1] \rightarrow X$  representing a point  $[\alpha] \in \widetilde{M}$ , and a chart  $(U_0, \phi_0)$  that contains the basepoint  $x_0$ . Now subdivide  $\alpha$  at points

$$x_0 = \alpha(t_0), x_1 = \alpha(t_1), \dots, x_n = \alpha(t_n)$$

where  $t_0 = 0$  and  $t_n = 1$  and so that each subpath  $\alpha: [t_i, t_{i+1}] \rightarrow X$  has image contained in a single chart  $(U_i, \phi_i)$ .

Now, at the  $i$ -th step, adjust the chart  $\phi_i$  by composing with  $\gamma_{(i-1),i}$ , so that it agrees with the previous (adjusted) chart. These form the *analytic continuation* of  $\phi_0$  along  $\alpha$ . The last chart is

$$\psi = \gamma_{01}(x_1)\gamma_{12}(x_2) \cdots \gamma_{(n-1),n}(x_n)\phi_n.$$

LEMMA 4.7. *Analytic continuation is well defined. That is, the germ of  $\psi$  at  $\alpha(1)$  does not depend on the choices of the  $t_i$  or the choice of  $\alpha$  in the homotopy class  $[\alpha] \in \widetilde{M}$ .*

PROOF. Exercise. □

We set  $\phi_0^{[\alpha]} = \psi$ , and by Lemma 4.7, the notation is well defined.

DEFINITION 4.8. For  $M$  a  $(G, X)$ -manifold with universal covering map  $\pi: \widetilde{M} \rightarrow M$ , fixed basepoint  $x_0 \in M$ , and fixed initial chart  $(U_0, \phi_0)$  about  $x_0$ , the *developing map*  $D: \widetilde{M} \rightarrow X$  is the map that agrees with the analytic continuation of  $\phi_0$  along each path, in a neighborhood of the path's endpoint. That is,

$$D = \phi_0^\sigma \circ \pi$$

in a neighborhood of  $\sigma \in \widetilde{M}$ .

Changing the basepoint and initial chart will change the developing map by composition with an element of  $G$  (exercise).

Now, if  $M$  has a  $(G, X)$ -structure, then so does  $\widetilde{M}$  (exercise). Under this  $(G, X)$  structure, the developing map becomes a local  $(G, X)$ -diffeomorphism between  $\widetilde{M}$  and  $X$ .

Consider the case that  $\sigma$  is an element of the fundamental group of  $M$ . Then  $\sigma$  is represented by a loop in  $M$ . Analytic continuation along a loop gives a germ  $\phi_0^\sigma$  that has domain a neighborhood of the basepoint of the loop. That is, we obtain a new chart defined in a neighborhood of the basepoint. Thus  $\phi_0^\sigma$  and  $\phi_0$  are both charts defined at the basepoint, and hence the maps differ by an element of  $G$ . Let  $g_\sigma \in G$  be the element such that  $\phi_0^\sigma = g_\sigma \phi_0$ .

It follows that

$$D \circ T_\sigma = g_\sigma \circ D,$$

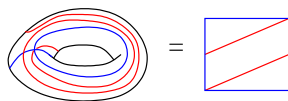


FIGURE 4.5. A nontrivial curve  $\gamma$  (red) on the torus. Meridian and longitude curves are shown in blue.

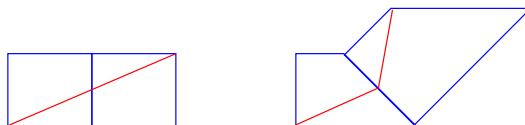


FIGURE 4.6. Left: developing a Euclidean torus. Right: developing an affine torus.

where  $T_\sigma$  is the covering transformation of  $\tilde{M}$  associated with  $\sigma$ . Apply this equation to a product. It follows that the map  $H: \pi_1(M) \rightarrow G$  defined by  $H(\sigma) = g_\sigma$  is a group homomorphism.

DEFINITION 4.9. The element  $g_\sigma$  is the *holonomy* of  $\sigma$ . The group homomorphism  $H$  is called the *holonomy* of  $M$ . Its image is the *holonomy group* of  $M$ .

Note that  $H$  depends on the choices from the construction of  $D$ . When  $D$  changes,  $H$  changes by conjugation in  $G$  (exercise).

EXAMPLE 4.10. Pick a point  $x$  on the torus, say  $x$  lies at the intersection of a choice of meridian and longitude curves for the torus, and consider a nontrivial curve  $\gamma$  based at  $x$ . An example of a nontrivial curve  $\gamma$  on the torus is shown in Figure 4.5.

Now consider a Euclidean structure on the torus. There exists a chart mapping  $x$  onto the Euclidean plane. We can take our chart to be an open parallelogram about  $x$ , where boundaries of the parallelogram glue in the usual way to form the torus. As the curve  $\gamma$  passes over a meridian or longitude, in the image of the developing map we must glue a new parallelogram to the appropriate side of the parallelogram we just left. See Figure 4.6, left, for an example. The tiling of the plane by parallelograms is the image of the developing map, or the developing image of the Euclidean torus.

As for the affine torus, Example 4.5, each time a curve crosses a meridian or longitude we attach a rescaled, rotated, translated copy of our quadrilateral to the appropriate edge. Figure 4.6 right shows an example. Figure 4.2 shows (part of) the developing image of the affine torus.

**4.2.2. Completeness of polygonal gluings.** Let  $M$  be an oriented hyperbolic surface obtained by gluing *ideal* hyperbolic polygons. An *ideal vertex* of  $M$  is an equivalence class of ideal vertices of the polygons, identified by the gluing. Let  $v$  be an ideal vertex, and let  $h$  be a horocycle centered at  $v$  on one of the polygons  $P$  incident to  $v$ . Now extend  $h$  counterclockwise

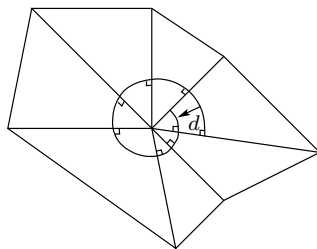


FIGURE 4.7. Extending a horocycle: view inside the manifold.

around  $v$  via the gluing. The horocycle  $h$  will meet a polygon glued to  $P$  in a right angle. Hence it will extend to a unique horocycle about  $v$  on that polygon as well. Continue. Eventually,  $h$  will return to  $P$ .

DEFINITION 4.11. Let  $d(v)$  denote the signed distance between  $h$  on  $P$  and the point on  $P$  where  $h$  re-enters  $P$  after extending it around  $v$ . See Figure 4.7. The sign is taken such that the direction shown in the figure is positive. Note  $d(v)$  does not depend on the initial choice of  $h$  (exercise).

It may be easier to compute  $d(v)$  if we look at polygons in  $\mathbb{H}^2$ , using terminology of developing map and holonomy.

Fix an ideal vertex on one of the polygons  $P$ . Put  $P$  in  $\mathbb{H}^2$  with  $v$  at infinity. Now take  $h$  to be a horocycle centered at infinity intersected with  $P$ . Follow  $h$  to the right. When it meets the edge of  $P$ , a new polygon is glued. The developing map instructs us how to embed that new polygon as a polygon in  $\mathbb{H}^2$ , with one edge the vertical geodesic which is the edge of  $P$ . Continue along  $h$ , placing polygons in  $\mathbb{H}^2$  according to their developing image. Eventually, the horocycle will meet  $P$  again. When this happens, the developing map will instruct us to glue a copy of  $P$  to the given edge. This copy of  $P$  will be isometric to the original copy of  $P$ , where the isometry is the holonomy of the closed path which encircles the ideal vertex once in  $v$  (why?). This holonomy element takes the horocycle  $h$  on our original copy of  $P$  to a horocycle  $h_0$ . The horocycle  $h_0$  will be of distance  $d(v)$  from the extension of  $h$ . See Figure 4.8.

PROPOSITION 4.12. *Let  $S$  be a surface with hyperbolic structure obtained by gluing hyperbolic polygons. Then the metric on  $S$  is complete if and only if  $d(v) = 0$  for each ideal vertex  $v$ .*

Before we prove this proposition, let's look at an example.

EXAMPLE 4.13 (Complete structures on the 3-punctured sphere). A topological polygonal decomposition for the 3-punctured sphere consists of two ideal triangles. See Figure 4.9.

Let's try to construct a geometric polygonal decomposition by building the developing image. We can put one of the ideal triangles in  $\mathbb{H}^2$  as the triangle with vertices at  $0, 1, \infty$ . If we glue the other triangle immediately

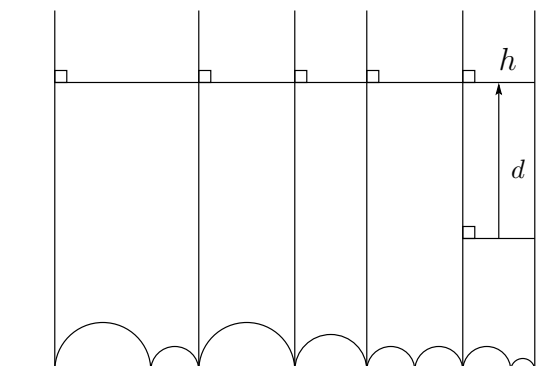


FIGURE 4.8. Extending a horocycle.

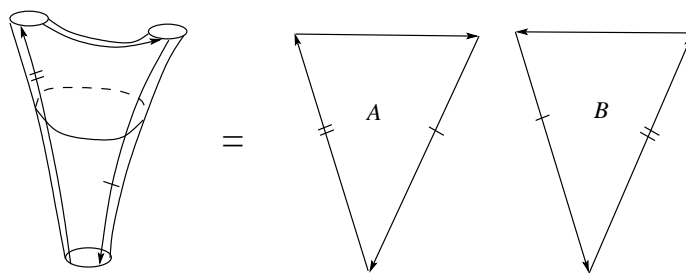
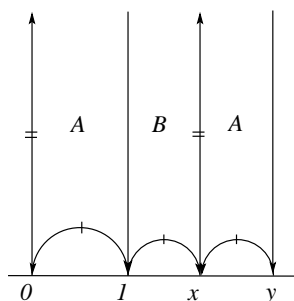


FIGURE 4.9. Topological polygonal decomposition for the 3-punctured sphere.

FIGURE 4.10. We may choose any  $x > 1$ ,  $y > x$  when finding a hyperbolic structure.

to the right, we have two vertices at 1 and at  $\infty$ , but the third can go to any point  $x$ , where  $x > 1$ . See Figure 4.10. These two triangles on the left, labeled  $A$  and  $B$ , give a fundamental region for the 3-punctured sphere. The developing image will be created by gluing additional copies of these two triangles to edges in the figure by holonomy isometries.

We may choose the position of the next copy of the triangle  $A$  glued to the right, putting its vertex at the point  $y$  as in Figure 4.10. After this

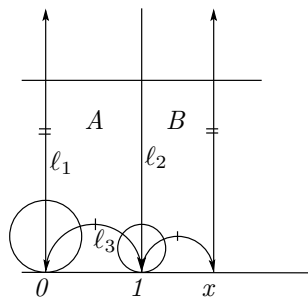


FIGURE 4.11.

choice, notice we cannot choose where the next vertex of  $B$  to the right will go. This is because the choice  $y$  determines an isometry of  $\mathbb{H}^2$  taking the triangle  $A$  on the left to the triangle labeled  $A$  on the right. This isometry is exactly the holonomy element corresponding to the closed curve running once around the vertex at infinity. The same isometry, which has been determined with the choice of  $y$ , must take  $B$  in the middle to the next triangle glued to the right in our figure. This is because the element of the fundamental group taking  $B$  in the middle to the next triangle on the right is exactly the same element of the fundamental group taking the triangle labeled  $A$  on the left to the one labeled  $A$  on the right. Thus the holonomy isometries must agree, and we cannot choose the next vertex of the triangle on the right. In fact, now that we know this holonomy element, we may apply it and its inverse successively to the triangles of Figure 4.10, and we obtain the entire developing image of all triangles adjacent to infinity.

Recall that we want our hyperbolic structure to be complete. By Proposition 4.12, we need to look at horocycles. Pick a collection of horocycles about the vertices  $0$ ,  $1$ , and  $\infty$ . Each of these horocycles extends to give a new horocycle about another copy of  $A$ . Each copy of  $A$  is obtained by applying a holonomy isometry to the original triangle with vertices at  $0$ ,  $1$ , and  $\infty$ . We want the horocycles obtained under these holonomy isometries to agree with the horocycles obtained by extending the original horocycles. This is the condition for completeness.

Here is a quick way to determine complete structures. Note that if the extended horocycles agree with the image of the horocycles under holonomy isometries, then the distances between horocycles will remain constant. Let the distance between horocycles be given by lengths  $l_1$ ,  $l_2$ , and  $l_3$  as in Figure 4.11.

If these lengths are to agree on each of the next copies of  $A$  under holonomy elements, then notice these lengths must agree on the triangle labeled  $B$ . Looking just at the vertical edges of  $B$ , one of them is already the appropriate length (that from  $1$  to  $\infty$ ). To make the other the correct length, the horocycle at the vertex  $x$  to be the same (Euclidean) size as that

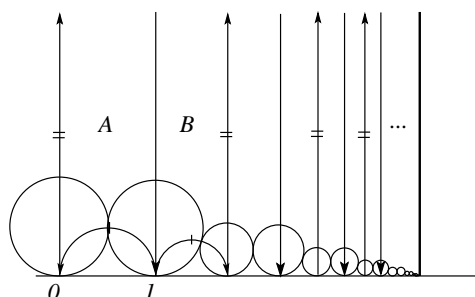


FIGURE 4.12. Part of developing image of an incomplete structure on a 3-punctured sphere.

at the vertex 0. But then the length of the third edge of  $B$  is determined. In order for this length to also be correct, we must set  $x = 2$ .

This analysis shows that there is exactly one complete structure on the 3-punctured sphere, a fundamental region for which is given by the two triangles with vertices  $0, 1, \infty$  and  $1, 2, \infty$ . Notice that the same discussion of lengths of edges will tell us exactly where to place each of the next triangles. We may create the entire developing image of the complete hyperbolic 3-punctured sphere by looking at lengths between horospheres.

EXAMPLE 4.14 (An incomplete structure on the 3-punctured sphere). What if we choose a different value for  $x$  besides  $x = 2$ ? Say we let  $x = 3/2$ . To simplify things, let's keep the length of the edge between horospheres at 0 and 1 constant as we extend horospheres. Choose horospheres at 0 and 1 of (Euclidean) radius  $1/2$ , so that these horospheres are tangent along the edge between 0 and 1, hence the length of the edge between horospheres is 0. We will keep the length of this edge 0 under each holonomy element. Then the horocycle about  $3/2$  must be tangent to the horocycle about 1, to keep the length between horospheres on this edge equal to 0. This determines where the next copy of the triangle  $A$  must go: its third vertex must have a horocycle about it of the same (Euclidean) size as the horocycle at  $3/2$ . This determines the holonomy isometry about the vertex at infinity. Apply this successively, and we obtain a pattern of triangles as in Figure 4.12.

Note the edges of the triangles approach a limit — the thick line shown on the far right of the figure. Notice this line is not part of the developing image of the 3-punctured sphere.

This hyperbolic structure is incomplete: a sequence of points running along a horocycle about infinity in  $\mathbb{H}^2$  projects to a Cauchy sequence that does not converge. Alternately, the value  $d(v)$  is nonzero for  $v$  the ideal vertex lifting to the point at infinity. The completion of this manifold is given by attaching a geodesic of length  $d(v)$ : each point of the geodesic corresponds to the limiting point of the Cauchy sequence given by a horocycle about infinity at the appropriate height. The triangles spiral around below this geodesic infinitely often, while horospheres head straight into it.

PROOF OF PROPOSITION 4.12. Suppose  $d(v)$  is nonzero. Then take a sequence of points on a horocycle about  $v$ . This gives a Cauchy sequence that does not converge. Therefore, the metric is not complete.

Now suppose  $d(v) = 0$  for each ideal vertex  $v$ . Then some horocycle closes up around each ideal vertex, so we may remove the interior horoball from each polygon. After this removal, the closure of the remainder is a compact manifold with boundary. For any  $t > 0$ , let  $S_t$  be the compact manifold obtained by removing interiors of horocycles of distance  $t$  from our original choice of horocycle. Then the compact subsets  $S_t$  of  $S$  satisfy  $\bigcup_{t \in \mathbb{R}^+} S_t = S$  and  $S_{t+a}$  contains a neighborhood of radius  $a$  about  $S_t$ . Any Cauchy sequence must be contained in some  $S_t$  for sufficiently large  $t$ . Hence by compactness of  $S_t$ , the Cauchy sequence must converge.  $\square$

### 4.3. Developing map and completeness

Here is a better condition for completeness that works in all dimensions and all geometries.

THEOREM 4.15. *Let  $M$  be an  $n$ -manifold with a  $(G, X)$ -structure, where  $G$  acts transitively on  $X$ , and  $X$  admits a complete  $G$ -invariant metric. Then the metric on  $M$  inherited from  $X$  is complete if and only if the developing map  $D: \widetilde{M} \rightarrow X$  is a covering map.*

PROOF. (C.f. Thurston [21, Proposition 3.4.15].) Suppose  $M$  is complete. To show  $D: \widetilde{M} \rightarrow X$  is a covering map, we show that any path  $\alpha_t$  in  $X$  lifts to a path  $\tilde{\alpha}_t$  in  $\widetilde{M}$ . Since  $D$  is a local homeomorphism, this implies that  $D$  is a covering map.

First, if  $M$  is complete, then  $\widetilde{M}$  must also be complete, where the metric  $\widetilde{M}$  is the lift of the metric on  $M$ , as follows. The projection to  $M$  of any Cauchy sequence gives a Cauchy sequence in  $M$ , with limit point  $x$ . Then  $x$  has a compact neighborhood which is evenly covered in  $\widetilde{M}$ , hence there is a compact neighborhood in  $\widetilde{M}$  containing all but finitely many points of the Cauchy sequence and also containing a lift of  $x$ . Thus the sequence converges in  $\widetilde{M}$ .

Let  $\alpha_t$  be a path in  $X$ . Because  $D$  is a local homeomorphism, we may lift  $\alpha_t$  to a path  $\tilde{\alpha}_t$  in  $\widetilde{M}$  for  $t \in [0, t_0)$ , some  $t_0 > 0$ . By completeness of  $\widetilde{M}$ , the lifting extends to  $[0, t_0]$ . But because  $D$  is a local homeomorphism, a lifting to  $[0, t_0]$  extends to  $[0, t_0 + \epsilon)$ . Hence the lifting extends to all of  $\alpha_t$  and  $D$  is a covering map.

The converse, which may be proved by similar methods, is Exercise 4.11.  $\square$

### 4.4. Exercises

EXERCISE 4.1. Fact: Up to rescaling, all Euclidean structures on a torus can be obtained by tiling the plane with parallelograms, and reading off

charts as in Example 4.4. We may take one of the parallelograms to have vertices at  $(0, 0)$ ,  $(1, 0)$ ,  $(p, q)$ , and  $(p + 1, q)$  for  $p > 0$ . Prove this fact.

EXERCISE 4.2. (Induced structures — Exercise 3.1.5 of Thurston [21]). Let  $\pi: N \rightarrow M$  be a local homeomorphism from a topological space  $N$  into a manifold  $M$  with a  $(G, X)$ -structure. Prove  $N$  has a  $(G, X)$ -structure so that  $\pi$  preserves the  $(G, X)$ -structure.

EXERCISE 4.3. Show that the following are equivalent for the manifold  $M$ .

- (a)  $M$  admits an  $(\text{Isom}(\mathbb{H}^2), \mathbb{H}^2)$ -structure.
- (b) For each point  $x$  in  $M$ , there exists a neighborhood  $U$  of  $x$  isometric to a ball in  $\mathbb{H}^2$ .

EXERCISE 4.4. Prove Claim 4.6. You may assume Exercise 4.3.

EXERCISE 4.5. Thurston [21, Exercise 3.4.1]. Prove Lemma 4.7. Also, determine how  $\phi_0^{[\alpha]}$  changes if we change the basepoint  $x_0$  or the initial chart  $\phi_0$ .

EXERCISE 4.6. Thurston [21, Exercise 3.4.3]. Compute developing maps and holonomies of a Euclidean and affine torus.

EXERCISE 4.7. Show  $d(v)$  is independent of initial choice of horocycle.

EXERCISE 4.8. How many incomplete hyperbolic structures are there on a 3-punctured sphere? How can they be parameterized? Give a geometric interpretation of this parameterization – i.e. relate the parameterization to the developing image of the associated hyperbolic structure.

EXERCISE 4.9. A torus with 1 puncture has a topological polygonal decomposition consisting of two triangles.

- (a) Find a complete hyperbolic structure on the 1-punctured torus and prove your structure is complete.
- (b) Find all complete hyperbolic structures on the 1-punctured torus. How are they parameterized?

EXERCISE 4.10. A sphere with 4 punctures has a topological polygonal decomposition consisting of four triangles. Find all complete hyperbolic structures on a 4-punctured sphere.

EXERCISE 4.11. Let  $M$  have a  $(G, X)$ -structure, where  $G$  acts transitively on  $X$ , and  $X$  is a complete  $G$ -invariant metric space. Prove that if the developing map  $D: \widetilde{M} \rightarrow X$  is a covering map, then  $M$  is complete under the metric inherited from  $X$ .

## CHAPTER 5

# Hyperbolic structures on knot complements

References for this section are Thurston’s book [21], and especially Thurston’s 1979 Princeton notes [19], particularly Chapter 4. In these notes, the example of the figure–8 knot is worked out in full detail (although you may find the language of that chapter confusing, the pictures are helpful).

### 5.1. Geometric triangulations

In the last set of notes, we defined topological and geometric polygonal decompositions of 2–manifolds. We can extend these notions to 3–manifolds. In the first set of notes, we obtained topological ideal polyhedral decompositions for knot complements. We can restrict further:

**DEFINITION 5.1.** Let  $M$  be a 3–manifold. A *topological ideal triangulation* of  $M$  is a combinatorial way of gluing truncated tetrahedra (ideal tetrahedra) so that the result is homeomorphic to  $M$ . Truncated parts will correspond to the boundary of  $M$ .

**EXAMPLE 5.2.** The figure–8 knot has a topological ideal triangulation consisting of two ideal tetrahedra, as we saw in exercise 7 of the first set of notes.

For a given knot complement, it is relatively easy to find topological ideal triangulations. Take any polyhedral decomposition, for example the one from the first set of notes. For each face of the polyhedral decomposition, pick an ideal vertex and subdivide the face into triangles with one vertex at the chosen ideal vertex. (Ensure that the same vertex is selected for faces that are glued, so the gluing extends to a gluing of triangles.) Now for each polyhedron, split off ideal tetrahedra by creating triangular faces.

**5.1.1. An extended example: the  $6_1$  knot.** We now work out an example for the  $6_1$  knot carefully. We will see how to decompose the complement into five tetrahedra. (In fact, the complement of the  $6_1$  knot can be decomposed into four tetrahedra, but we won’t bother simplifying further here.)

We start with a polyhedral decomposition of the  $6_1$  knot. We use the decomposition obtained using the methods of Chapter 2. The result is shown in Figure 5.1, with the knot on the left, the top polyhedron in the center (viewed from inside), and the bottom polyhedron on the left (viewed from outside).

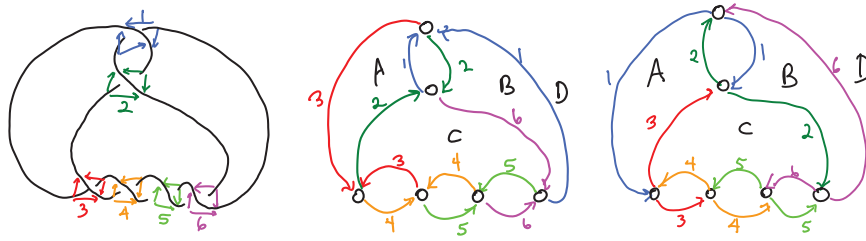


FIGURE 5.1. Left: The  $6_1$  knot. Middle: Top polyhedron (from inside). Right: Bottom polyhedron (from outside).

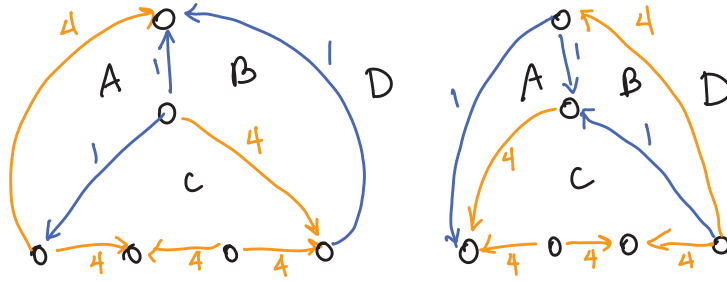


FIGURE 5.2. Left: Top polyhedron with no bigons (from inside). Right: Bottom polyhedron with no bigons (from outside).

The next step is to collapse all bigons. When we do so, edges in Figure 5.1 labeled 2 become edges labeled 1 with opposite orientation. Edges 3, 5, and 6 are collapsed to edge 4, with 3 and 5 switched to 4 with the opposite orientation, and 6 switched to 4 with the same orientation. The result is shown in Figure 5.2.

Now subdivide faces  $C$  and  $D$  into triangles. We subdivide those on the top first. Note this forces the subdivision of  $C$  and  $D$  on the bottom, to match the top. One choice of subdivision is shown in Figure 5.3.

Next we split these polyhedra into tetrahedra, by cutting off tetrahedra chunks. That is, cut along a new face to split the polyhedra into tetrahedra. We do two such moves on the top polyhedron. These are shown in Figures 5.4 and 5.5.

Now we split the bottom polyhedron into smaller chunks, by cutting along triangular faces, splitting off four ideal vertices at a time. We perform two cuts on the bottom polyhedron, shown in Figures 5.6 and 5.7.

Notice that the polyhedron on the left in Figure 5.7 is not a tetrahedron: the edges labeled 7 and 10 in that polyhedron form a bigon, which collapses to a single edge which we label 7. When we do the collapse, the faces  $E_4$  and  $D_2$  collapse to a single triangle, which we will label  $D_2$ . The faces  $E_3$  and

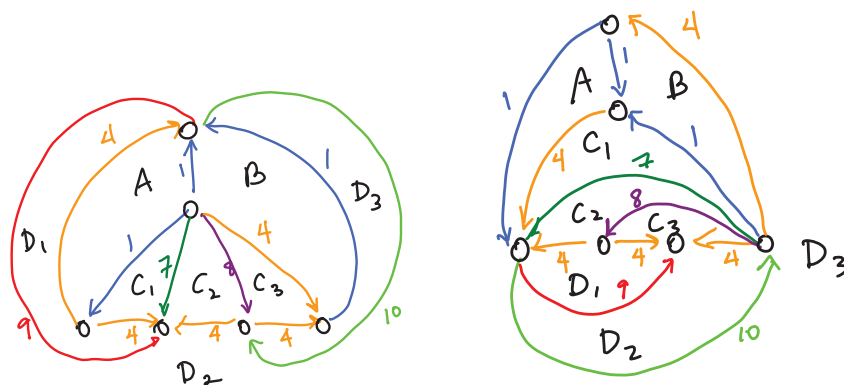


FIGURE 5.3. A subdivision of faces  $C$  and  $D$  in the top polyhedron (left) leads to a subdivision of the bottom (right)

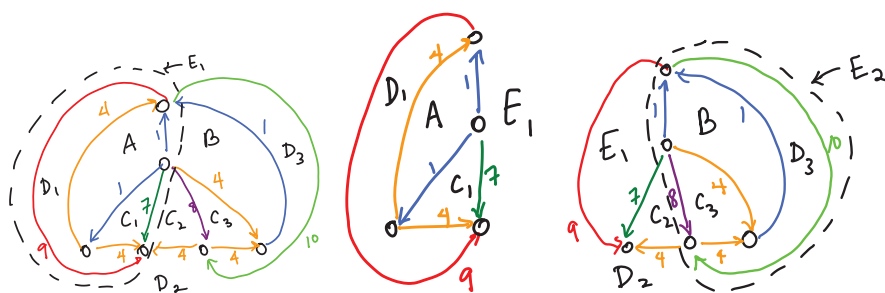


FIGURE 5.4. Cut along a new face  $E_1$  (dashed on the left) to split polyhedron into one tetrahedron (middle) and another ideal polyhedron (right). We will cut the polyhedron on the right along the face  $E_2$ .

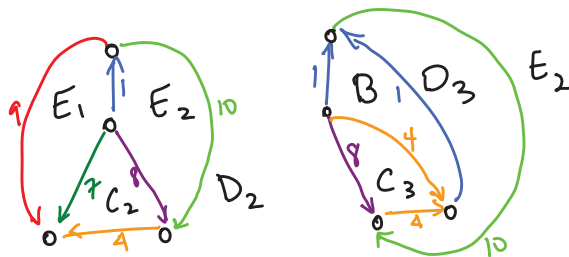


FIGURE 5.5. Cut the polyhedron on the right of Figure 5.4 along the face  $E_2$  to split it into the two tetrahedra shown above.

$D_3$  also collapse to a single triangle, which we will label  $D_3$ . The resulting tetrahedra are shown in Figure 5.8.

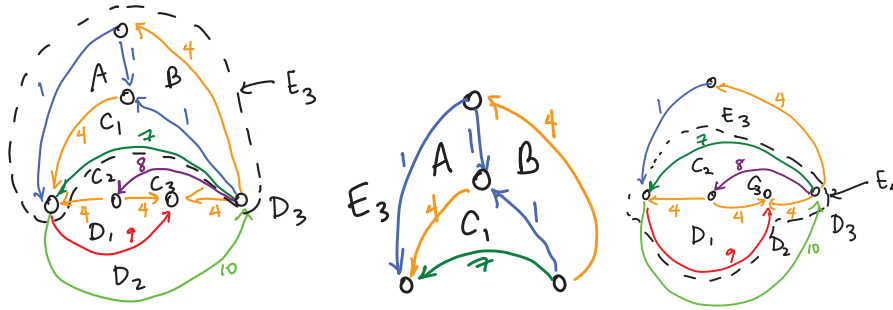


FIGURE 5.6. Cut the bottom polyhedron along a triangle  $E_3$  on left, splitting into two polyhedra shown middle and right. We will next cut along the triangle  $E_4$  shown on right.

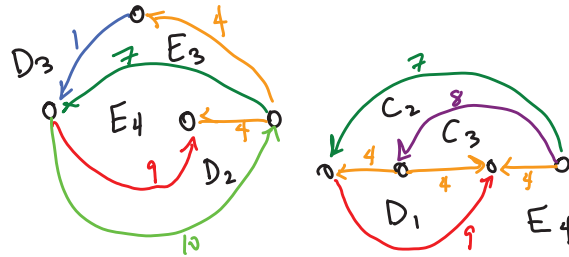


FIGURE 5.7. Cutting along  $E_4$  in Figure 5.6 yields the two polyhedra shown above.

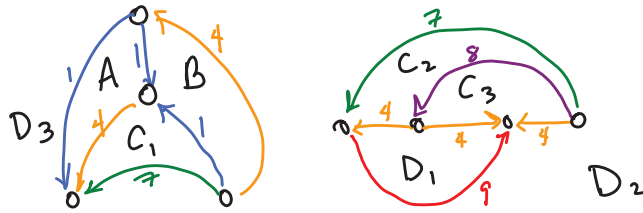


FIGURE 5.8. Two tetrahedra remain from the original bottom polyhedron after collapsing degenerate polyhedra.

When we have finished, we have five tetrahedra that glue to give the complement of the  $6_1$  knot. All five tetrahedra with their edges and faces labeled are shown in Figure 5.9.

### 5.1.2. Geometric ideal triangulations.

DEFINITION 5.3. A *geometric ideal triangulation* of  $M$  is a topological ideal triangulation such that each tetrahedron has a geometric structure, and the result of gluing is a smooth manifold with a complete metric.

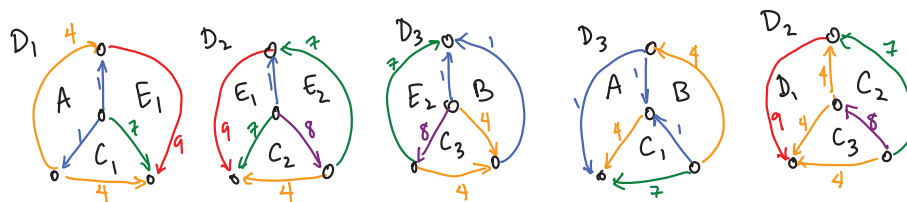


FIGURE 5.9. Five tetrahedra which glue to give the complement of the  $6_1$  knot.

We will eventually see that every hyperbolic 3-manifold  $M$  has a geometric ideal polyhedral decomposition, called the canonical polyhedral decomposition. However, subdividing this decomposition into tetrahedra may create degenerate tetrahedra — actual topological tetrahedra (as opposed to the object labeled (5) in example 5.1.1), but tetrahedra that are flat or negatively oriented in the hyperbolic structure on  $M$ .

The following questions are unknown (i.e. you may do a final project on any of them). They are listed in decreasing order of generality.

OPEN PROBLEM 5.4. *Does every hyperbolic manifold have a geometric ideal triangulation?*

OPEN PROBLEM 5.5. *Does every hyperbolic knot complement have a geometric ideal triangulation?*

OPEN PROBLEM 5.6. *Does every complement of a hyperbolic alternating knot have a geometric ideal triangulation?*

As far as I am aware, only 2-bridge knots are known to have a geometric ideal triangulation.

OPEN PROBLEM 5.7. *Prove that for some other large class of knots, all knots in the class have a geometric ideal triangulation.*

## 5.2. Gluing equations

In the 3rd set of notes, we saw that a gluing of polygons has a hyperbolic structure if and only if the angle sum around each finite vertex is  $2\pi$  (in exercise). There are similar conditions for a gluing of hyperbolic tetrahedra. We now need to consider gluing around an edge. First, consider edges of ideal tetrahedra.

Any ideal tetrahedron has six edges. Recall: If we select any one, say  $e$ , we may put the endpoints of  $e$  at 0 and  $\infty$ , send a third vertex to 1, and the fourth vertex will be some  $z' \in \mathbb{C}$ . We may assume that  $z'$  has positive imaginary part, for if not, apply an isometry of  $\mathbb{H}^3$  rotating around the geodesic from 0 to  $\infty$  and rescaling so that  $z'$  maps to 1. The image of 1 under this isometry will be the desired complex number. For the edge  $e$ , define the number  $z(e) \in \mathbb{C}$  to be the complex number with positive

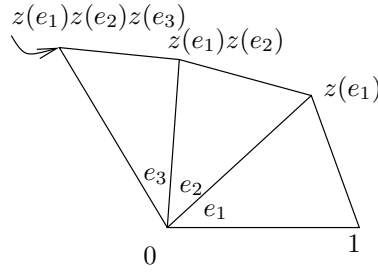


FIGURE 5.10. Vertices of attached triangles.

imaginary part we obtain from this process. This is called the *edge invariant* of  $e$ .

Now consider a gluing of ideal tetrahedra. Fix an edge  $e$  of the gluing, and let  $T_1$  be a tetrahedron which has edge  $e_1$  glued to  $e$ . Put  $T_1$  in  $\mathbb{H}^3$  with the edge  $e_1$  running from 0 to  $\infty$ , with a third vertex at 1, and the fourth vertex at  $z(e_1)$ , where  $z(e_1)$  has positive imaginary part. The gluing identifies each face of  $T_1$  with another face. Let  $F_1$  denote the face of  $T_1$  with vertices 0,  $z(e_1)$ , and  $\infty$ . This is glued to a face  $F'_1$  in some tetrahedron  $T_2$ , where the edge  $e_2$  in  $T_2$  glues to  $e$ .

Now, we could put  $T_2$  in  $\mathbb{H}^3$  with vertices at 0,  $\infty$ , 1, and  $z(e_2)$ , but since we're gluing to  $T_1$ , we want the face  $F'_1$  to have vertices 0,  $\infty$ , and  $z(e_1)$  rather than vertices 0,  $\infty$ , and 1. Thus to do the gluing, we apply an isometry of  $\mathbb{H}^3$  fixing 0 and  $\infty$ , mapping 1 to  $z(e_1)$ . This takes the fourth vertex of  $T_2$  to  $z(e_1)z(e_2)$ .

Continue attaching tetrahedra counterclockwise around  $e$ . The next tetrahedron attached will have vertices 0,  $\infty$ ,  $z(e_1)z(e_2)$ , and  $z(e_1)z(e_2)z(e_3) \in \mathbb{C}$ . See Figure 5.10. Eventually one of the tetrahedra will be glued to  $T_1$  again. The fourth vertex of the final tetrahedron will be at  $z(e_1)z(e_2) \cdots z(e_n)$ .

**THEOREM 5.8** (Gluing equations). *Let  $M^3$  admit a topological ideal triangulation such that each ideal tetrahedron has a hyperbolic structure. The hyperbolic structures on the ideal tetrahedra induce a hyperbolic structure on the gluing,  $M$ , if and only if for each edge  $e$ ,  $\prod z(e_i) = 1$  and  $\sum \arg(z(e_i)) = 2\pi$ , where the product and sum are over edges that glue to  $e$ .*

**PROOF.** The hyperbolic structure on the tetrahedra induces a hyperbolic structure on  $M$  if and only if every point in  $M$  has a neighborhood isometric to a ball in  $\mathbb{H}^3$ . Consider a point on an edge. If it has a neighborhood isometric to a ball in  $\mathbb{H}^3$  then the sum of the dihedral angles around the edge must be  $2\pi$ . See Figure 5.11. This sum of dihedral angles is  $\sum \arg(z(e_i))$ . Moreover there must be no nontrivial translation as we move around the edge. Since the last face of the last triangle glues to the triangle with vertices 0, 1, and  $\infty$ , this condition requires that  $\prod z(e_i) = 1$ .

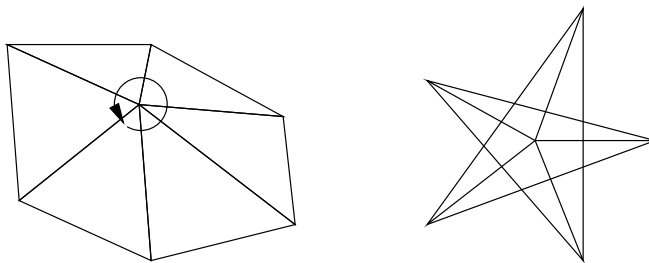


FIGURE 5.11. Left: Angle sum must be  $2\pi$ . Right: An example of why this condition is important.

Conversely, if we have  $\prod z(e_i) = 1$  and  $\sum \arg(z(e_i)) = 2\pi$ , then the developing image around the edge gives a smooth hyperbolic structure.  $\square$

The equations  $\prod z(e_i) = 1$  (and restrictions  $\sum \arg(z(e_i)) = 2\pi$ ) are called the *gluing equations*. We have one for each edge.

How many hyperbolic structures does this give us? Each ideal tetrahedron has six edges. Are there  $6t$  unknowns in the gluing equations, where  $t$  is the total number of tetrahedra? No — we can determine the number of unknowns for each tetrahedron by applying Möbius transformations.

(This was exercise (3.8) in Chapter 3 of the notes, but nobody did it in class.)

Put edge  $e_1$  running from 0 to  $\infty$ , with a third vertex at 1 and the fourth vertex at  $z$ . The edge invariant  $z(e_1) = z$ . Let  $e_2$  be the edge running from 1 to  $\infty$ . What is its edge invariant? To determine  $z(e_2)$ , we apply a Möbius transformation fixing  $\infty$ , taking 1 to 0, and taking  $z$  to 1. This transformation is given by

$$w \mapsto \frac{w-1}{z-1}.$$

It sends 0 to  $-1/(z-1)$ . Thus  $z(e_2) = 1/(1-z)$ .

As for the edge  $e_3$  running from  $z$  to  $\infty$ , to determine its edge invariant we apply a Möbius transformation fixing  $\infty$ , sending  $z$  to 0, and sending 0 to 1. This is given by

$$w \mapsto \frac{w-z}{-z}.$$

It sends 1 to  $(1-z)/(-z)$ . Thus  $z(e_3) = (z-1)/z$ .

Summarizing, we have:

$$(1) \quad z(e_1) = z \quad z(e_2) = \frac{1}{1-z} \quad z(e_3) = \frac{z-1}{z}$$

Note we have the following relationships for these edge invariants.

$$z(e_1)z(e_2)z(e_3) = -1$$

$$1 - z(e_1) + z(e_1)z(e_3) = 0$$

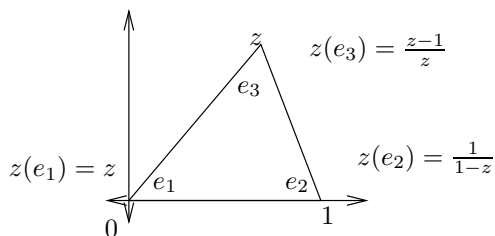


FIGURE 5.12. Edge invariants

Finally, the tetrahedron has three additional edges. By the proof of part (b) of exercise (7) from the notes part 2, opposite edges have identical edge invariants. Thus one ideal tetrahedron contributes at most one unknown to the gluing equations.

EXAMPLE 5.9 (Gluing equations for figure–8 knot). We saw in the first set of notes that the figure–8 knot decomposes into two ideal tetrahedra. Choose the two tetrahedra to be *regular*. That is, all dihedral angles are  $\pi/3$ . We claim that this gives a hyperbolic structure on the figure–8 knot complement.

We wish to find all such structures.

Thurston worked through this example in detail in his notes [19, pages 50–52]. We recall his work here.

Figure 5.13 is from page 51 of [19]. This shows the two tetrahedra in the decomposition of the figure–8 knot complement, which we obtained in Chapter 2. These tetrahedra differ from ours in the following ways. First, the bottom tetrahedron agrees with ours, except that all edges have been reversed. The top doesn't look like ours because in Chapter 2, recall that we created the top polyhedron with our head on the inside. To get Thurston's picture, we need to move our head to the outside. This reflects the polyhedron. After a rotation, we see that the decomposition agrees with ours.

Note there are two edge classes in the tetrahedra in Figure 5.13, labelled with one or two lines on the edge. However, each tetrahedron has three complex numbers,  $z_1, z_2, z_3$  and  $w_1, w_2, w_3$ , respectively, which will give gluing consistency equations. We read these off of the two edges.

For the edge with one line through it, we have:

$$z_1^2 z_2 w_1^2 w_2 = 1.$$

For the edge with two lines:

$$z_3^2 z_2 w_3^2 w_2 = 1.$$

We set  $z_1 = z$  and  $w_1 = w$ . From equations (1), we obtain:

$$z^2 \left( \frac{z-1}{z} \right) w^2 \left( \frac{w-1}{w} \right) = 1,$$

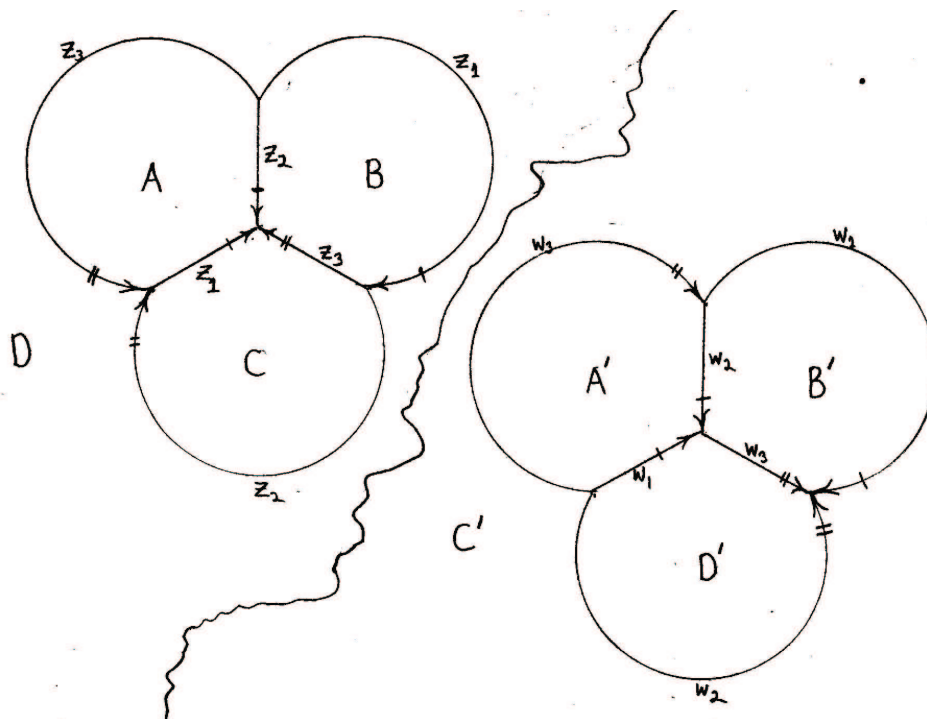


FIGURE 5.13. The ideal tetrahedra of the Figure-8 knot, from [19].

or

$$z(z-1)w(w-1) = 1.$$

Solve for  $z$  in terms of  $w$ :

$$(2) \quad z = \frac{1 \pm \sqrt{1 + 4/(w(w-1))}}{2}.$$

We need the imaginary parts of  $z$  and  $w$  to be strictly greater than 0. For each value of  $w$ , there is at most one solution for  $z$  with positive imaginary part. The solution exists provided that the discriminant  $1 + 4/(w(w-1))$  is not positive real. Solutions are parameterized by the region of  $\mathbb{C}$  shown in Figure 5.14.

Notice that

$$z = w = \sqrt[3]{-1} = \frac{1}{2} + \frac{\sqrt{3}}{2}i$$

is a solution to the equations. We will see that this gives a complete hyperbolic structure on the complement of the Figure-8 knot.

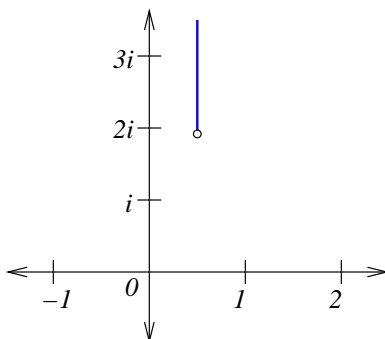


FIGURE 5.14. Solutions to gluing equations for the Figure–8 knot complement are parametrized by the above region.

### 5.3. Completeness equations

DEFINITION 5.10. Let  $M$  be a 3–manifold with torus boundary. Define a *cuspidal neighborhood* of  $M$  to be a neighborhood of  $\partial M$  homeomorphic to a torus cross an interval.

A hyperbolic structure on  $M$  induces an affine structure on the boundary of any cusp of  $M$ .

THEOREM 5.11. *Let  $M$  be a 3–manifold with hyperbolic structure, i.e. with  $(\text{Isom}(\mathbb{H}^3), \mathbb{H}^3)$ –structure. Then the structure on  $M$  is complete if and only if for each cusp of  $M$ , the induced structure on the boundary of the cusp is a Euclidean structure on the torus.*

PROOF. Exercise. □

DEFINITION 5.12. If  $M$  has a topological ideal triangulation, then by looking at truncated vertices of the corresponding ideal tetrahedra we obtain a triangulation of each boundary torus. Call this a *cuspidal triangulation*.

Let  $M$  be a 3–manifold which admits a topological ideal triangulation and a hyperbolic structure on each tetrahedron such that the structure satisfies the gluing equations of Theorem 5.8. Let  $T$  be the boundary of a cusp of  $M$ , and let  $\alpha \in \pi_1(T)$ . We may associate a complex number  $H(\alpha)$  to  $\alpha$  as follows.

ALGORITHM 5.13. Lift the cuspidal triangulation to the universal cover. Fix a directed edge  $e$  of the triangulation. Some covering transformation  $T_\alpha$  takes the directed edge to another directed edge. Two directed edges may be connected by a path through the triangulation, where each step of the path is rotation around some vertex of a triangle, taking the edge of the triangle to the other edge of the triangle through that vertex, preserving the given direction on the edge.

Now, each vertex of the cuspidal triangulation corresponds to an edge of the triangulation, hence has an associated edge invariant. To obtain  $H(\alpha)$ , do the following algorithm.

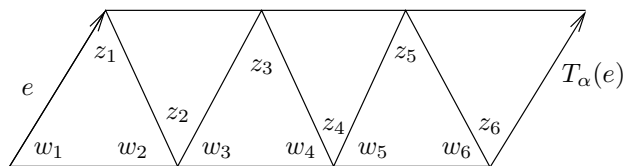


FIGURE 5.15. Figure of Example 5.14.

Start with  $H = 1$

- If the next step of the path is a counterclockwise rotation about a vertex with associated edge invariant  $z$ , then replace  $H$  by  $zH$ .
- If instead the next step is clockwise rotation about a vertex with associated edge invariant  $z$ , replace  $H$  by  $H/z$ .

At the end of the path, if the direction on the edge obtained by the path of rotations does not match the direction of  $T_\alpha(e)$ , then replace  $H$  with  $-H$ .

Set  $H(\alpha) = H$ .

EXAMPLE 5.14. If  $e$  and  $T_\alpha(e)$  are as shown in Figure 5.15, then  $H(\alpha)$  is given by

$$H(\alpha) = z_1 z_2^{-1} z_3 z_4^{-1} z_5 z_6^{-1}.$$

Alternately, we have

$$H(\alpha) = w_1^{-1} w_2^{-1} z_2^{-1} w_3^{-1} w_4^{-1} z_4^{-1} w_5^{-1} w_6^{-1} z_6^{-1} (-1).$$

You should check that these give the same complex number, using relationships between edge invariants in a single triangle.

PROPOSITION 5.15. *Let  $T$  be the torus boundary of a cusp neighborhood of  $M$ , where  $M$  admits a topological ideal triangulation, and the ideal tetrahedra admit hyperbolic structures that satisfy the gluing equations (Theorem 5.8). Let  $\alpha$  and  $\beta$  generate  $\pi_1(T)$ . If  $H(\alpha) = H(\beta) = 1$ , then the ideal triangulation is a geometric ideal triangulation.*

In other words, the hyperbolic structure on  $M$  induced by the hyperbolic structures on the tetrahedra will be a complete structure. The equations  $H(\alpha) = 1$  and  $H(\beta) = 1$  are called the *completeness equations*.

PROOF SKETCH. By Theorem 5.11, it suffices to show that the induced structure on  $T$  is Euclidean. To show this, we need to show that  $T_\alpha$  and  $T_\beta$  are pure translations. Since  $H(\alpha) = 1$ , the edge  $e$  is not rotated by  $T_\alpha$ , nor is its length scaled. Thus  $T_\alpha$  is a pure translation, so an isometry of  $\mathbb{E}^2$ . Similarly for  $T_\beta$ . Then the holonomy group of  $T$  is generated by pure translations, hence the induced structure on  $T$  is Euclidean.  $\square$

EXAMPLE 5.16. The figure-8 knot complement has a complete hyperbolic structure if and only if triangulation extends to give a Euclidean structure on the torus at infinity. Thurston finds the triangulation of the cusp on page 53 of [19]. He shows how to obtain completeness equations on page 54.

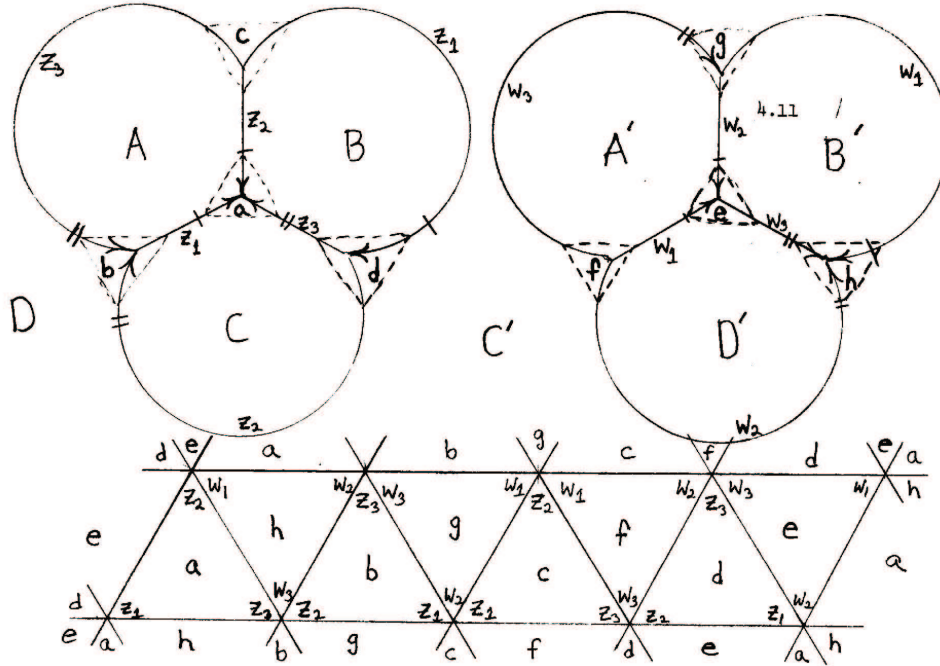


FIGURE 5.16. Finding the cusp triangulation of the Figure-8 knot complement, from page 53 of [19].

We include his figures here.

First, finding the cusp triangulation, in Figure 5.16. Note we draw a small triangle around each ideal vertex of the tetrahedra, then follow through the gluing of the faces of the tetrahedra to determine how these smaller triangles glue up.

Next, we find the completeness equations. This is done in Figure 5.17. We use generators  $x$  and  $y$  shown in that figure, and the algorithm given above.

Following that figure, we find that

$$H(x) = z_1^2(w_2w_3)^2 = \left(\frac{z}{w}\right)^2$$

$$(3) \quad H(y) = \frac{w_1}{z_3} = w(1-z).$$

If the hyperbolic structure is complete, then by Proposition 5.15,  $H(x) = H(y) = 1$ , so  $z = w$ . From equation (2),  $(z(z-1))^2 = 1$ . From equation (3),  $z(z-1) = -1$ . Hence the only possibility is  $z = w = \sqrt[3]{-1}$ .

### 5.4. Exercises

EXERCISE 5.1. Write down the gluing equations (not completeness equations) for the  $6_1$  knot, using the ideal tetrahedra of the handwritten example

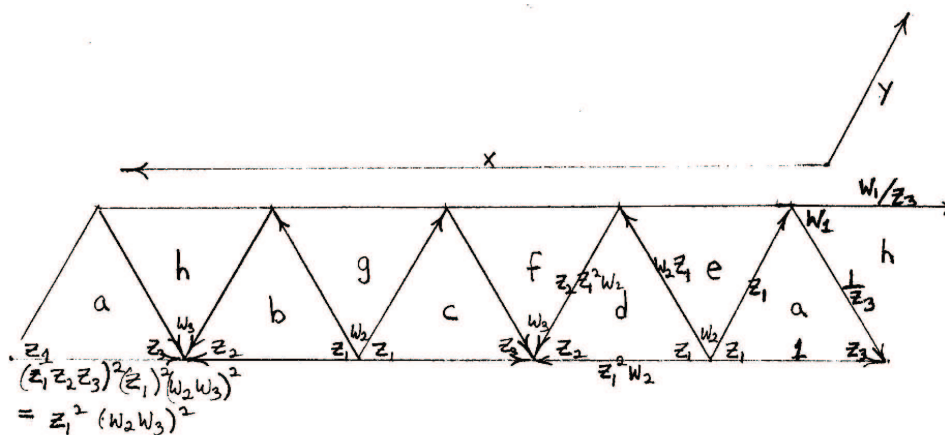


FIGURE 5.17. Finding the completeness equations for the Figure-8 knot, from page 54 of [19].

5.1.1. Make appropriate substitutions such that your equations contain exactly one variable per tetrahedron.

EXERCISE 5.2. Notice that for both the figure-8 knot complement and for the  $6_1$  knot, we had exactly the same number of edges as tetrahedra in the ideal triangulation.

- Prove that this will always be true. That is, prove that if  $M$  is any 3-manifold with (possibly empty) boundary consisting of tori, then for any topological ideal triangulation of  $M$ , the number of edges of the triangulation will always equal the number of tetrahedra.
- Since we have one unknown per ideal tetrahedra, part (a) implies that the number of gluing equations will equal the number of unknowns. However, in fact the gluing equations are always redundant. Prove this fact.

EXERCISE 5.3. In notes 1, we found a polyhedral decomposition of the  $5_2$  knot complement (without bigons).

- By adding edges and faces, split this into a topological ideal triangulation of the knot complement.
- Write down all edge parameters and all gluing equations, one variable per tetrahedron.

EXERCISE 5.4. Find a topological ideal triangulation of the  $6_3$  knot, edge parameters, and gluing equations.

EXERCISE 5.5. For the topological triangulation of the  $5_2$  knot of exercise 5.3:

- Find the triangulation of the cusp. Label a fundamental domain, and meridian and longitude.

(b) Write down completeness equations.

EXERCISE 5.6. Find the cusp triangulation for the complement of the  $6_1$  knot from Example 5.1.1.

EXERCISE 5.7. Find completeness equations for the  $6_1$  knot.

EXERCISE 5.8. Find completeness equations for the  $6_3$  knot.

EXERCISE 5.9. Prove Theorem 5.11.

EXERCISE 5.10. What breaks down when you try to follow this procedure for non-hyperbolic knots and links, such as the trefoil or the  $(2, 4)$ -torus link?

## CHAPTER 6

# Completion and Dehn filling

In this chapter, we examine completions of incomplete hyperbolic structures.

### 6.1. Mostow–Prasad rigidity

In Chapter 4 in the exercises, we found 2-parameter families of complete hyperbolic structures on the punctured torus and on the 4-punctured sphere. This flexibility is only possible in two dimensions. In higher dimensions, there is only *one* complete structure on a finite volume hyperbolic manifold, up to isometry. This result is known as Mostow–Prasad rigidity.

**THEOREM 6.1** (Mostow–Prasad rigidity, algebraic version). *Suppose  $\Gamma_1$  and  $\Gamma_2$  are two discrete subgroups of the group of isometries of  $\mathbb{H}^n$ ,  $n \geq 3$ , such that  $\mathbb{H}^n/\Gamma_i$  has finite volume, and suppose  $\phi: \Gamma_1 \rightarrow \Gamma_2$  is a group isomorphism. Then  $\Gamma_1$  and  $\Gamma_2$  are conjugate subgroups.*

View  $\mathbb{H}^n$  as the universal cover of  $M_i = \mathbb{H}^n/\Gamma_i$ , with  $\Gamma_i$  the fundamental group of  $M_i$ . Then if  $\Gamma_1$  and  $\Gamma_2$  are conjugate, then the manifolds  $\mathbb{H}^n/\Gamma_1$  and  $\mathbb{H}^n/\Gamma_2$  are isometric.

**THEOREM 6.2** (Mostow–Prasad rigidity, geometric version). *If  $M_1^n$  and  $M_2^n$  are complete hyperbolic manifolds with finite volume, any isomorphism of fundamental groups  $\phi: \pi_1(M_1) \rightarrow \pi_1(M_2)$  is realized by a unique isometry.*

We aren't going to cover the proof of this theorem in this class. Thurston sketches a proof in section 5.9 in his notes [19]. A more complete proof is contained in the book by Benedetti and Petronio [3], Chapter C.

The theorem says that any complete hyperbolic structure we find on a knot or link complement, or any  $n$ -manifold with finite volume, is the *only* complete structure, provided  $n$  is at least 3. This is one reason hyperbolic geometry makes nice knot invariants.

### 6.2. Completion of incomplete structures on hyperbolic manifolds

Good references for this section again include Benedetti and Petronio [3, Chapter E]. Cooper, Hodgson, and Kerckhoff also have a nice book that describes carefully different behavior of the completion of various incomplete manifolds [4]. Ratcliffe also works through this in detail [15, Section 10.5].

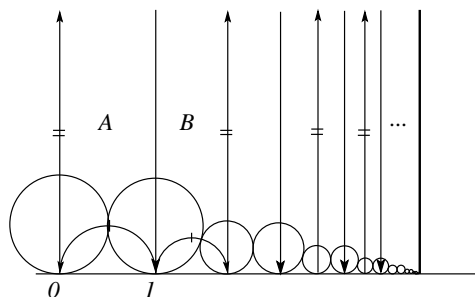


FIGURE 6.1. Incomplete structure on a 2-manifold.

What about incomplete structures on a manifold with torus boundary? There are lots of these. For the figure–8 knot complement, for example, we found a 1-complex parameter family of incomplete structures, parameterized by  $w \in \mathbb{C}$  with  $\text{Im}(w) > 0$ . If we take the *completion* of a hyperbolic structure on a 3-manifold, we obtain surprising topological results.

**6.2.1. 2-manifolds.** As a warm up, let’s consider completions of incomplete structure on 2-manifolds. In Chapter 4, we saw an example of an incomplete structure on a hyperbolic 3-punctured sphere. Recall that in the developing map for an incomplete structure, ideal polygons approached a limiting line. By selecting a point on a horocycle about infinity, approaching this line, we obtained a Cauchy sequence that did not converge. See Figure 4.12.

Now take the completion of this hyperbolic structure. We will need to adjoin a point on a horocycle, so that this Cauchy sequence will converge. Note we will need to adjoin a single point for each distinct horocycle. Recall also the invariant  $d(v)$  — the distance between a horocycle and its translate under the holonomy of the curve going around the ideal vertex. Notice that horocycles of distance  $d(v)$  apart will be identified, and so to form the completion of the manifold, we adjoin a single point for all of these.

In total: we will adjoin a segment of the limiting line of length  $d(v)$  to our manifold to form the completion. This attaches a geodesic. Ideal triangles spiral around the geodesic, never quite reaching it, but horocycles run straight into the geodesic, meeting it and edges of ideal triangles at right angles along the way. See Figure 6.2.

**6.2.2. 3-manifolds.** We learned in Chapter 5 that if a hyperbolic structure on a triangulated 3-manifold with torus boundary is *not* complete, then for an ideal vertex  $v$ , the holonomy of  $\text{link}(v)$  acts on a horosphere by affine, not Euclidean transformations. Thus  $\text{link}(v)$  inherits an affine, but not Euclidean, structure in the incomplete case. (Recall  $\text{link}(v)$  is the boundary of a neighborhood about  $v$ . In Exercise 6.7 you will show  $\text{link}(v)$  is always a torus.)

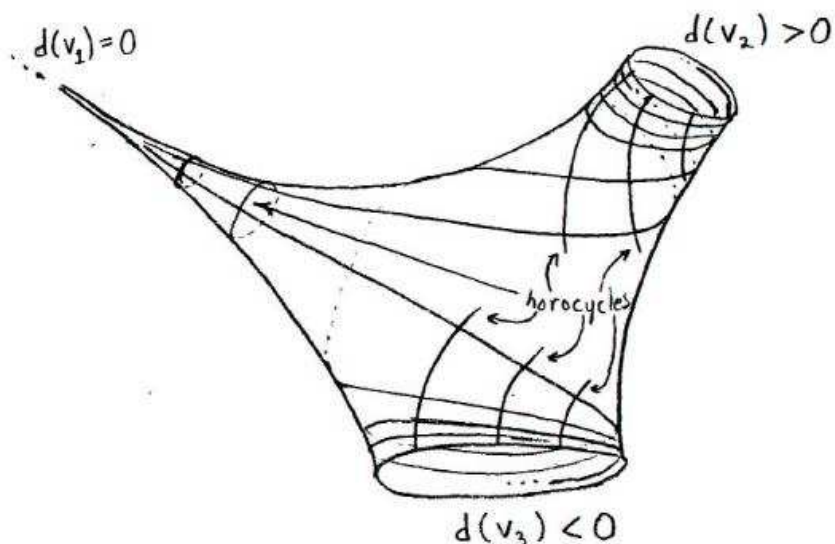


FIGURE 6.2. An example of the completion of a hyperbolic 2-manifold. This figure is from [19].

Let  $\alpha$  and  $\beta$  generate  $\pi_1(\text{link}(v)) \cong \mathbb{Z} \times \mathbb{Z}$ . Corresponding to  $\alpha$  and  $\beta$  are two holonomy isometries. We will abuse notation slightly and refer to these isometries as  $\alpha$  and  $\beta$ . Assume the action of  $\alpha$  and  $\beta$  does not induce a Euclidean structure on  $\text{link}(v)$ , so the hyperbolic structure on  $M$  is not complete. To form its completion, we remove a small neighborhood  $N(v)$  of  $v$ , take the completion of  $N(v)$ , and then reattach it to  $M$ . We need to analyze what this neighborhood looks like.

Consider the developing map for the affine torus  $\text{link}(v)$ . The image will miss single point, and will look something like the developing image of the affine torus shown in Figure 4.2 in Chapter 4. This image is obtained by considering the action of  $\alpha$  and  $\beta$  restricted to a horosphere. More precisely, if  $M$  has an ideal polyhedral decomposition, then we build its developing image by starting with an ideal polyhedron in  $\mathbb{H}^3$ , lifting so that  $\infty$  projects to  $v$ . Intersect the polyhedron with a horosphere about infinity. This gives a Euclidean polygon on the horosphere. Now the gluing map (developing map) tells us exactly how to glue polyhedra to the original polyhedron. The horosphere intersects these attached polyhedra in new polygons, glued to the first. Just by intersecting polyhedra with polygons, we obtain the developing image of  $\text{link}(v)$ . Notice that the holonomy for this restriction to the selected horosphere is generated by  $\alpha$  and  $\beta$  alone: only the gluing maps about the cusp come into play. Others move us away from the horosphere about infinity.

If we shift the original choice of horosphere up, we will see the same image of the developing map on polyhedra. In particular, the developing

map will still miss a single point, with the same complex value for each choice of horosphere. These missed points form a vertical geodesic in  $\mathbb{H}^3$ . We may apply an isometry so that this vertical geodesic runs from 0 to  $\infty$  in  $\mathbb{H}^3$ . Let  $N(v)$  denote a neighborhood of the ideal vertex  $v$ . By shrinking  $N(v)$ , if necessary, the above shows that the developing image of  $N(v)$  misses the single geodesic from 0 to  $\infty$  in  $\mathbb{H}^3$ .

Clearly the completion of  $N(v)$  is obtained by adjoining (some portion of) this geodesic. As in the case of incomplete 2-manifolds, the length of the adjoined geodesic will be determined by considering the action of the holonomy. Note  $\alpha$  and  $\beta$  act on the geodesic from 0 to  $\infty$ . Since points in our completion should be identified to their images under the holonomy action, we should identify each point  $z$  on the geodesic from 0 to  $\infty$  with  $\langle \alpha, \beta \rangle \cdot z$ . There are two cases.

**Case 1.** The image of  $z$  under the action of  $\alpha$  and  $\beta$  is dense in the line from 0 to  $\infty$ . In this case, the completion is the one-point compactification. It is not a manifold. (Exercise.)

**Case 2.** The image of  $z$  is a discrete set of points on the line, each of some distance  $d(v)$  apart. Then the completion is obtained by adjoining a geodesic circle of length  $d(v)$  to  $N(v)$ . Denote the completion by  $\bar{N}(v)$ . We wish to understand the topology and geometry of  $\bar{N}(v)$ .

Let  $\zeta \in \pi_1(\text{link}(v))$  generate the kernel of the action of  $\pi_1(\text{link}(v))$  on the line from 0 to  $\infty$ . The isometry  $\zeta$  will be a rotation about this line by some angle  $\theta$ . Now a perpendicular cross section of the circle added to  $\bar{N}(v)$  to form the completion will be a hyperbolic cone, of cone angle  $\theta$ . This makes sense even when  $\theta > 2\pi$ .

When we attach  $\bar{N}(v)$  back to  $M$ , the result  $\bar{M}$  is called a *hyperbolic cone manifold*. Its *cone angle* is  $\theta$ . The added geodesic circle in  $\bar{M}$  is the *singular locus* of  $\bar{M}$ . Note the hyperbolic metric on  $\bar{M}$  is smooth everywhere except at points on the singular locus.

When  $\theta = 2\pi$ , the hyperbolic metric on  $\bar{M}$  is now actually smooth everywhere. Thus  $\bar{M}$  is some hyperbolic manifold. However,  $\bar{M}$  will not be homeomorphic to  $M$ .

We may obtain a manifold homeomorphic to  $M$  by removing a small, closed tubular neighborhood of the singular locus in  $\bar{M}$ . Notice that a tubular neighborhood of a circle is a solid torus. Since the singular locus in  $\bar{M}$  is a circle, a tubular neighborhood of it is homeomorphic to a solid torus. Thus we obtain a manifold homeomorphic to  $\bar{M}$  by attaching a solid torus to a torus boundary component of  $M$ .

**DEFINITION 6.3.** Let  $M$  be a manifold with torus boundary component  $T$ . Let  $s$  be an isotopy class of simple closed curves on  $T$ . The manifold obtained from  $M$  by attaching a solid torus to  $T$  so that  $s$  bounds a disk in the resulting manifold is called the *Dehn filling of  $M$  along  $s$*  and is denoted  $M(s)$ .

Conclusion: when the holonomy  $\rho(\pi_1(\text{link}(v)))$  acts on the geodesic omitted from its developing image by a fixed translation, and when the generator  $\zeta \in \pi_1(\text{link}(v))$  of the kernel is a rotation by  $2\pi$ , then the completion of  $M$  is a complete hyperbolic manifold, homeomorphic to the Dehn filled manifold  $M(\zeta)$ .

### 6.3. Hyperbolic Dehn surgery space

We re-interpret the above section in the language of complex lengths of isometries of  $\mathbb{H}^3$ .

Anytime  $M$  admits a hyperbolic structure and a decomposition into hyperbolic ideal polyhedra, we can show  $\text{link}(v)$  is a torus for each ideal vertex  $v$  (exercise). The fundamental group of the torus is isomorphic to  $\mathbb{Z} \times \mathbb{Z}$ , generated by some  $\alpha$  and  $\beta$ . (When  $M$  is a knot complement, it is standard to choose  $\alpha$  to be the meridian, i.e. a curve bounding a disk in  $S^3$ , and  $\beta$  to be the longitude, i.e. the curve homologous to 0 in  $M$ .) Consider the holonomy elements of  $\alpha$  and  $\beta$ . These are some isometries of  $\mathbb{H}^3$ . As above, we will continue to abuse notation and denote the holonomy isometries corresponding to  $\alpha$  and  $\beta$  by  $\alpha$  and  $\beta$ .

Recall the classification of isometries of  $\mathbb{H}^3$ . Any isometry is one of three types:

- (1) Parabolic, with a single fixed point on the boundary at infinity. When we conjugate such that the fixed point is at infinity, these are translations  $z \mapsto z + a$  for some  $a \in \mathbb{C}$ .
- (2) Elliptic, fixing two points on the boundary at infinity. Conjugating such that the two fixed points are 0 and  $\infty$ , this is a rotation about the geodesic from 0 to  $\infty$ . The geodesic fixed by the rotation is called the *axis* of the isometry.
- (3) Loxodromic, or hyperbolic. Again there are two fixed points on the boundary at infinity, but the isometry translates and rotates along the geodesic between them. This geodesic is again called the *axis* of the isometry.

Since  $\alpha$  and  $\beta$  generate  $\mathbb{Z} \times \mathbb{Z}$ , they must commute. This is possible only if  $\alpha$  and  $\beta$  are parabolic, fixing the same point at infinity, or if  $\alpha$  and  $\beta$  share the same axis (exercise).

If  $\alpha$  and  $\beta$  are parabolic, fixing a point at infinity, then they must fix an entire horosphere about infinity. Conjugating to put their fixed point at  $\infty$  in  $\partial\mathbb{H}^3$ , they are of the form  $\alpha(z) = z + a$ ,  $\beta(z) = z + b$ . Hence they restrict to Euclidean isometries on the horosphere, and the hyperbolic structure is complete.

Now consider incomplete structures. In this case, because  $\alpha$  and  $\beta$  commute but are not parabolic, they share an axis, and are both given by rotation and/or translation along this axis. In particular, the axis must be exactly the vertical geodesic whose points are omitted from the developing image of  $\text{link}(v)$  for each horosphere.

DEFINITION 6.4. Fix a direction on the axis of  $\alpha$  and  $\beta$ . Any element  $\gamma$  of  $\pi_1(\text{link}(v))$  translates some signed distance  $d$  along the axis, and rotates by total angle  $\theta \in \mathbb{R}$ , where the sign of  $\theta$  is given by the right hand rule. Let  $\mathcal{L}(\gamma) = d + i\theta$ . The value  $\mathcal{L}(\gamma)$  is called the *complex length* of  $\gamma$ . This defines a function  $\mathcal{L}$  from  $\pi_1(\text{link}(v)) = H_1(\text{link}(v); \mathbb{Z})$  to  $\mathbb{C}$ .

Notice that if  $\gamma = p\alpha + q\beta$ , then  $\mathcal{L}(\gamma) = p\mathcal{L}(\alpha) + q\mathcal{L}(\beta)$ , so  $\mathcal{L}$  is a linear map. We may extend it canonically to a linear map  $\mathcal{L}: H_1(\text{link}(v); \mathbb{R}) \rightarrow \mathbb{C}$ . The value  $\mathcal{L}(c)$  for any  $c \in H_1(\text{link}(v); \mathbb{R}) \cong \mathbb{R}^2$  will be called the complex length of  $c$ .

Suppose that the complex length of a simple closed curve  $\gamma$  on  $T = \text{link}(v)$  equals  $2\pi i$ . Then in the completion of  $M$ ,  $\gamma$  will bound a smooth hyperbolic disk. This implies that the completion of  $M$  is a manifold homeomorphic to the Dehn filled manifold  $M(\gamma)$ , and that  $M(\gamma)$  admits a complete hyperbolic structure.

Suppose instead that the complex length of a closed curve  $\gamma$  on  $T$  equals  $\theta i$ . Then in the completion of  $M$ ,  $\gamma$  will bound a hyperbolic cone, with cone angle  $\theta$ . The completion of  $M$  is still homeomorphic to the Dehn filled manifold  $M(\gamma)$  (since a hyperbolic cone is homeomorphic to a disk). However, the metric on  $M(\gamma)$  inherited from the completion of  $M$  is not smooth. The core of the added solid torus is the singular locus, with cone angle  $\theta$ .

Most generally, there will be a unique element  $c \in H_1(T; \mathbb{R})$  so that  $\mathcal{L}(c) = 2\pi i$ .

DEFINITION 6.5. We say  $c \in H_1(T; \mathbb{R})$  such that  $\mathcal{L}(c) = 2\pi i$  is the *Dehn surgery coefficient* of the boundary component  $T = \text{link}(v)$ .

When  $c$  is of the form  $(p, q)$ , with  $p$  and  $q$  relatively prime integers, it corresponds to a simple closed curve and the completion is smooth.

We have been looking at a fixed incomplete hyperbolic structure on  $M$ , and examining possible completions for this fixed structure. Now we turn our attention to a topological manifold  $X$ , homeomorphic to  $M$ , and consider all possible hyperbolic structures on  $X$ .

DEFINITION 6.6. Let  $X$  be a 3-manifold with boundary component  $T$ . The subset of  $H_1(T; \mathbb{R})$  consisting of Dehn surgery coefficients of hyperbolic structures on  $X$  is called the *hyperbolic Dehn surgery space* for  $X$ .

If  $X$  admits a complete hyperbolic structure, then we let  $\infty$  correspond to the complete hyperbolic structure on  $X$ .

THEOREM 6.7 (Thurston's hyperbolic Dehn filling theorem). *Suppose  $X$  is a 3-manifold with boundary a single torus  $T$ , such that  $X$  admits a complete hyperbolic structure. Then hyperbolic Dehn surgery space for  $X$  always contains an open neighborhood of  $\infty$ .*

*More generally, if  $X$  has torus boundary components  $T_1, \dots, T_n$ , and admits a complete hyperbolic structure, then the hyperbolic Dehn surgery space for  $X$  contains an open neighborhood of  $\infty$  for each  $T_i$ .*

The proof of Theorem 6.7 is sketched in Thurston’s notes [19], and done carefully in Benedetti and Petronio for triangulated 3–manifolds [3]. Precise, universal bounds on the size of that open neighborhood of  $\infty$  were given by Hodgson and Kerckhoff [7], about 25 years after Theorem 6.7 was proved. With the resolution of the geometrization conjecture, this result can also be proved by using results of Agol and Lackenby [1, 9], and then applying geometrization. (All the proofs require work.)

**COROLLARY 6.8.** *Let  $X$  be a manifold with torus boundary that admits a complete hyperbolic metric. Then there are at most finitely many Dehn fillings of  $X$  which do not admit a complete hyperbolic metric.*

**COROLLARY 6.9.** *Let  $X$  be a manifold with torus boundary components  $T_1, \dots, T_n$ . For each  $T_i$ , exclude finitely many Dehn fillings. Remaining Dehn fillings yield a manifold with a complete hyperbolic structure.*

Notice that Corollary 6.9 does not rule out the fact that a manifold may have infinitely many non-hyperbolic Dehn fillings. For example, the Whitehead link complement admits a complete hyperbolic structure. The trivial Dehn filling on one gives an unknotted circle in  $S^3$ . Any Dehn filling of this result will be a lens space, which is not hyperbolic (exercise). So there are infinitely many non-hyperbolic Dehn fillings. However, Corollary 6.9 does imply that these non-hyperbolic Dehn fillings are more rare than hyperbolic ones.

The following is sometimes called the Fundamental Theorem of Wallace and Lickorish. It was proved independently by Wallace and Lickorish in the early 1960’s. A nice, highly readable proof can be found in Rolfsen’s book [16].

**THEOREM 6.10** (Fundamental theorem of Wallace and Lickorish). *Let  $M$  be a closed, orientable 3–manifold. Then  $M$  is obtained by Dehn filling the complement of a link in  $S^3$ .*

Moreover, again work of Thurston implies we may actually take the complement of the link in  $S^3$  of Theorem 6.10 to admit a complete hyperbolic structure. Thus Thurston’s theorem on Dehn fillings, along with Wallace and Lickorish’s theorem implies that, in some sense, “almost all” 3–manifolds are hyperbolic.

**OPEN PROBLEM 6.11.** *What is the topology of hyperbolic Dehn surgery space? For example, is it connected? Is it path connected? That is, if a finite volume manifold  $M(s)$  admits a complete hyperbolic structure, and if  $M$  also admits a complete hyperbolic structure, is there necessarily a smooth deformation of the hyperbolic structure running from the complete structure on  $M$  to the complete structure on  $M(s)$ ? Is it star shaped? That is, if  $M(s)$  admits a complete hyperbolic structure, and  $M$  admits a complete hyperbolic structure, can we deform the hyperbolic structure on  $M$  through cone manifolds with cone angles increasing monotonically from 0 (at the complete structure on  $M$ ) to  $2\pi$  (at the complete structure on  $M(s)$ )?*

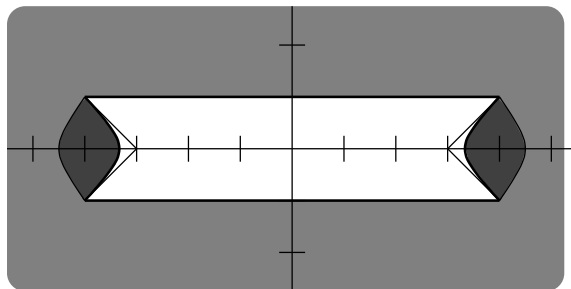


FIGURE 6.3. Hyperbolic Dehn surgery space for the figure-8 knot complement is known to include the lightly shaded region, is conjectured to contain the darkly shaded regions, and is conjectured to contain no other points.

We don't even know if hyperbolic Dehn filling space is connected for the simplest of examples — the figure-8 knot complement. Thurston did identify part of the boundary of the neighborhood about infinity separating hyperbolic Dehn fillings from non-hyperbolic ones. This is done on pages 58 through 61 of his notes [19]. To determine these boundaries, he considers what is happening to the two hyperbolic structures on the tetrahedra as the values of their edge invariants approach the boundaries given by the gluing equations (the boundaries of the region in Figure 5.14). When both tetrahedra degenerate, the hyperbolic structure collapses and the limiting manifold is not hyperbolic.

However, when only one tetrahedron degenerates, we still have a hyperbolic structure for a little while. In this case, we will be gluing a positively oriented tetrahedron to a negatively oriented one. We can make sense of this by cutting the negatively oriented tetrahedron into pieces and subtracting them from the positively oriented one, leaving a polyhedron  $P$ . Faces of  $P$  may then be identified to give a hyperbolic structure. No one knows exactly where this stops working, although Hodgson's 1986 PhD thesis [6] gives evidence that the boundary should be as shown in Figure 6.3.

In Exercise 6.1, you are asked to study how tetrahedra degenerate in the figure-8 knot complement.

**OPEN PROBLEM 6.12.** *Completely characterize hyperbolic Dehn surgery space for the figure-8 knot complement. See Figure 6.3.*

Dehn fillings that do not yield a hyperbolic manifold are called *exceptional*. There are still many open problems on exceptional Dehn fillings.

For example, no hyperbolic manifold can contain an embedded 2-sphere that does not bound a 3-ball (exercise). A manifold that contains such a 2-sphere is called *reducible*. If you start with a hyperbolic 3-manifold, perform Dehn filling, and obtain a reducible manifold, the Dehn filling is called *reducible*.

OPEN PROBLEM 6.13 (The cabling conjecture). *No hyperbolic knot complement admits a reducible Dehn filling.*

The original wording of the cabling conjecture was that only cables of knots admitted reducible Dehn fillings. The conjecture listed as Open Problem 6.13 is the only remaining case to prove. A solution of the problem will probably involve hyperbolic geometry of knot complements, maybe including an examination of the surfaces sitting inside the knot complement.

A related open problem concerns lens spaces. Note lens spaces are another class of non-hyperbolic manifolds (exercise). There is no way to put a complete hyperbolic metric on a lens space.

OPEN PROBLEM 6.14 (The Berge conjecture). *If Dehn filling on a knot produces a lens space, then the knot is a Berge knot.*

Berge knots were studied by John Berge. These knots can be characterized as follows. Give  $S^3$  its standard genus-2 Heegaard splitting. That is, a standardly embedded genus 2 surface in  $S^3$  splits  $S^3$  into two handlebodies. Let  $K$  be a curve on the genus 2 surface which is a generator of the fundamental group of both handlebodies. Then  $K$  is a Berge knot.

Up until 2008, I could have put the Gordon conjecture on this list. Gordon conjectured that the maximal number of exceptional Dehn fillings on a hyperbolic 3-manifold with one cusp is exactly 10. This was proved, by a computer assisted proof, by Lackenby and Meyerhoff [10]. However, the following related conjecture still remains open:

OPEN PROBLEM 6.15. *The figure-8 knot is the only hyperbolic 3-manifold which admits the maximal number of exceptional Dehn fillings. That is, there is no hyperbolic 3-manifold besides the figure-8 knot complement which admits 10 exceptional Dehn fillings.*

## 6.4. Exercises

EXERCISE 6.1 (Incomplete structures on the figure-8 knot). In Thurston's notes, page 52, a figure showing all parameterizations of hyperbolic structures on the figure-8 knot is given. For any  $w$  in this region, formula 4.3.2 in the notes gives us a corresponding  $z$  so that if two tetrahedra with edge invariants  $z$  and  $w$  are glued, we obtain a (possibly incomplete) hyperbolic structure on the figure-8 knot.

Analyze what happens to the tetrahedra corresponding to  $z$  and to  $w$  as  $w$  approaches a point on the boundary of this region.

More specifically, if  $w$  approaches certain points on the boundary of this region, tetrahedra corresponding to both  $z$  and  $w$  start to become degenerate. Which points are these? Prove that the two tetrahedra are becoming degenerate in this case.

As  $w$  approaches other values on the boundary, only one of the tetrahedra degenerates. Which points are these? Prove that only one tetrahedron is degenerating in this case.

- EXERCISE 6.2. (a) Let  $g$  be a geodesic in  $\mathbb{H}^3$ , and let  $p$  be a point on the boundary at infinity of  $\mathbb{H}^3$ , disjoint from the endpoints of  $g$ . Prove there exists a unique geodesic running from  $p$ , perpendicular to  $g$ .
- (b) Let  $g_1$  and  $g_2$  be geodesics in  $\mathbb{H}^3$  with disjoint endpoints on the boundary at infinity of  $\mathbb{H}^3$ . Prove there exists a unique geodesic perpendicular to both  $g_1$  and  $g_2$ .

EXERCISE 6.3. Given an incomplete structure on a 3-punctured sphere, find a decomposition of the completion of the structure into hyperbolic polygons. Note the original decomposition of the 3-punctured sphere into two ideal triangles will not work: it does not include any geodesics attached in the completion.

EXERCISE 6.4. We have seen that the completion of an incomplete hyperbolic 3-manifold is no longer homeomorphic to the original hyperbolic 3-manifold. Is this true for completions of incomplete structures on the 3-punctured sphere? What surface do we obtain when we complete an incomplete hyperbolic structure on a 3-punctured sphere? Prove it.

EXERCISE 6.5. Let  $A$  and  $B$  in  $\mathrm{PSL}(2, \mathbb{C})$  be distinct from the identity. Prove that the following are equivalent.

- (a)  $A$  and  $B$  commute.
- (b) Either  $A$  and  $B$  have the same fixed points, or  $A$  and  $B$  have order 2 and each interchanges the fixed points of the other.
- (c) Either  $A$  and  $B$  are parabolic with the same fixed point at infinity, or the axes of  $A$  and  $B$  coincide, or  $A$  and  $B$  have order 2 and their axes intersect orthogonally in  $\mathbb{H}^3$ .

EXERCISE 6.6. Suppose  $M$  is a closed manifold with a complete hyperbolic structure. Prove that  $\pi_1(M)$  cannot contain a  $\mathbb{Z} \times \mathbb{Z}$  subgroup. Conclude that  $M$  cannot contain an embedded torus  $T$  such that  $\pi_1(T)$  injects into  $M$ . [Such a torus is called *incompressible*. A Dehn filling resulting in a closed manifold with an embedded incompressible torus is another example of an exceptional filling.]

EXERCISE 6.7. Let  $M$  be an orientable 3-manifold with a decomposition into ideal polyhedra, each with a hyperbolic structure, such that the polyhedra induce a hyperbolic structure on  $M$ . Let  $v$  be an ideal vertex of  $M$ , i.e. an equivalence class of ideal vertices of the polyhedra, where vertices are equivalent if and only if they are identified under the gluing of the polyhedra.

Recall that  $\mathrm{link}(v)$  is defined to be the boundary of a neighborhood of  $v$  in  $M$ .

- (a) Prove  $\mathrm{link}(v)$  always inherits a similarity structure from the hyperbolic structure on  $M$ . Here a similarity structure is a  $(\mathrm{Sim}(\mathbb{E}^2), \mathbb{E}^2)$ -structure, where  $\mathrm{Sim}(\mathbb{E}^2)$  is a subgroup of the group of affine transformations consisting of elements of the form  $x \mapsto Ax + b$ , where

$A$  is a linear map that rotates and/or scales only. Thus  $\text{Sim}(\mathbb{E}^2)$  is formed by rotations, scalings, and translations.

- (b) Prove that the only closed, orientable surface which admits a similarity structure is a torus. It follows that  $\text{link}(v)$  is always homeomorphic to a torus when  $M$  is an orientable manifold with hyperbolic structure (even incomplete).

EXERCISE 6.8. Let  $M$  be an orientable 3-manifold with a decomposition into ideal polyhedra, each with a hyperbolic structure, such that the gluing induces an incomplete hyperbolic structure on  $M$ , and the completion is the one-point compactification of a neighborhood  $N(v)$  of an ideal vertex  $v$ . Prove that the completion is not a manifold.

EXERCISE 6.9. Prove that a reducible manifold cannot be hyperbolic. That is, it admits no complete hyperbolic structure.

EXERCISE 6.10. Prove that a lens space cannot admit a complete hyperbolic structure.

EXERCISE 6.11 (On complex length of  $A$  in  $\text{PSL}(2, \mathbb{C})$ ). (a) Suppose

$A \in \text{PSL}(2, \mathbb{C})$  has axis the geodesic from  $0$  to  $\infty$ . Then the matrix of  $A$  may be parameterized by a single complex number  $\lambda$ . What is the form of this matrix?

- (b) Denote the trace of a matrix  $A$  by  $\text{tr}(A)$ , and its complex length by  $\mathcal{L}(A)$ . Prove that  $\text{tr}(A) = 2 \cosh(\mathcal{L}(A)/2)$ .



## Bibliography

- [1] Ian Agol, *Bounds on exceptional Dehn filling*, *Geom. Topol.* **4** (2000), 431–449. [61]
- [2] James W. Anderson, *Hyperbolic geometry*, second ed., Springer Undergraduate Mathematics Series, Springer-Verlag London Ltd., London, 2005. [19]
- [3] Riccardo Benedetti and Carlo Petronio, *Lectures on hyperbolic geometry*, Universitext, Springer-Verlag, Berlin, 1992. [55, 61]
- [4] Daryl Cooper, Craig D. Hodgson, and Steven P. Kerckhoff, *Three-dimensional orbifolds and cone-manifolds*, *MSJ Memoirs*, vol. 5, Mathematical Society of Japan, Tokyo, 2000, With a postface by Sadayoshi Kojima. [55]
- [5] Cameron McA. Gordon and John Luecke, *Knots are determined by their complements*, *J. Amer. Math. Soc.* **2** (1989), no. 2, 371–415. [6]
- [6] Craig D. Hodgson, *Degeneration and regeneration of geometric structures on 3-manifolds*, Ph.D. thesis, Princeton Univ., 1986. [62]
- [7] Craig D. Hodgson and Steven P. Kerckhoff, *Universal bounds for hyperbolic Dehn surgery*, *Ann. of Math. (2)* **162** (2005), no. 1, 367–421. [61]
- [8] Jim Hoste, Morwen Thistlethwaite, and Jeff Weeks, *The first 1,701,936 knots*, *Math. Intelligencer* **20** (1998), no. 4, 33–48. [6]
- [9] Marc Lackenby, *Word hyperbolic Dehn surgery*, *Invent. Math.* **140** (2000), no. 2, 243–282. [61]
- [10] Marc Lackenby and Robert Meyerhoff, *The maximal number of exceptional Dehn surgeries*, *Invent. Math.* **191** (2013), no. 2, 341–382. [63]
- [11] A. Marden, *Outer circles*, Cambridge University Press, Cambridge, 2007, An introduction to hyperbolic 3-manifolds. [19, 22]
- [12] William W. Menasco, *Polyhedra representation of link complements*, *Low-dimensional topology* (San Francisco, Calif., 1981), *Contemp. Math.*, vol. 20, Amer. Math. Soc., Providence, RI, 1983, pp. 305–325. [9]
- [13] G. D. Mostow, *Strong rigidity of locally symmetric spaces*, Princeton University Press, Princeton, N.J., 1973, *Annals of Mathematics Studies*, No. 78. [6]
- [14] Gopal Prasad, *Strong rigidity of  $\mathbf{Q}$ -rank 1 lattices*, *Invent. Math.* **21** (1973), 255–286. [6]
- [15] John G. Ratcliffe, *Foundations of hyperbolic manifolds*, second ed., *Graduate Texts in Mathematics*, vol. 149, Springer, New York, 2006. [19, 55]
- [16] Dale Rolfsen, *Knots and links*, Publish or Perish Inc., Berkeley, Calif., 1976, *Mathematics Lecture Series*, No. 7. [61]
- [17] Peter Scott, *The geometries of 3-manifolds*, *Bull. London Math. Soc.* **15** (1983), no. 5, 401–487. [5]
- [18] Dan Silver, *Knot theory’s odd origins*, *American Scientist* **94** (2006), no. 2, 158 – 165. [5]
- [19] William P. Thurston, *The geometry and topology of three-manifolds*, Princeton Univ. Math. Dept. Notes, 1979, Available at <http://www.msri.org/communications/books/gt3m>. [2, 9, 23, 28, 41, 48, 49, 51, 52, 53, 55, 57, 61, 62]
- [20] ———, *Three-dimensional manifolds, Kleinian groups and hyperbolic geometry*, *Bull. Amer. Math. Soc. (N.S.)* **6** (1982), no. 3, 357–381. [5, 6]

- [21] ———, *Three-dimensional geometry and topology. Vol. 1*, Princeton Mathematical Series, vol. 35, Princeton University Press, Princeton, NJ, 1997, Edited by Silvio Levy. [2, 9, 19, 27, 32, 39, 40, 41]

# Index

- $(G, X)$ -structure, 27
- $d(v)$ , 33
- affine torus, 29
- alternating, 12
- ambient isotopic, 4
- analytic continuation, 31
- bigon, 14
- chart, 27
- complete hyperbolic surface, 33
- complete structure, 37
- completeness equations, 49
- complex length, 58
- cone angle, 56
- cone manifold, 56
- coordinate change, 27
- cross ratio, 21
- cuspidal neighborhood, 48
- cuspidal triangulation, 48
- Dehn filling, 56
- Dehn surgery coefficient, 58
- developing map, 31
- elliptic, 57
- Euclidean structure, 27
- exceptional Dehn fillings, 60
- geometric ideal triangulation, 42
- geometric polygonal decomposition, 27
- gluing, 27
- holonomy, 32
- holonomy group, 32
- horoball, 19, 20
- horocycle, 18
- horosphere, 20
- hyperbolic cone manifold, 56
- hyperbolic Dehn surgery space, 58
- hyperbolic structure, 29
- ideal polyhedron, 7
- ideal tetrahedron, 20
- ideal triangle, 18
- ideal vertex, 32
- incomplete 3-punctured sphere, 36
- incompressible torus, 62
- knot, 4
- knot complement, 4
- knot diagram, 7
- knot invariant, 5
- link, 4
- link invariant, 5
- loxodromic, 57
- Mostow–Prasad rigidity, 53
- nugatory crossing, 14
- parabolic, 57
- polyhedron, 7
- reducible, 60
- reducible Dehn filling, 60
- singular locus, 56
- topological ideal triangulation, 39
- topological polygonal decomposition, 27
- transition map, 27